RESEARCH ARTICLE

Title

- **Dual Recognition of Multiple Signals in Bacterial Outer Membrane Proteins Enhance Assembly and Maintain Membrane Integrity**
- **Short title: OMP assembly is dependent on multiple recognition signals**

Authors

Edward M. Germany[1,2], Nakajohn Thewasano[1,2], Kenichiro Imai[3], Yuki Maruno[1,2], Rebecca S. Bamert[4,5], Christopher J. Stubenrauch[4,5], Rhys A. Dunstan[4,5], Yue Ding[6,7], Yukari Nakajima[1,2], XiangFeng Lai[6], Chaille T. Webb[4,5], Kentaro Hidaka[1,2], Kher Shing Tan[4,5], Hsin-Hui Shen[6,7,*], Trevor Lithgow[4,5,*], and Takuya Shiota[1,2,*]

Affiliations

[1]Frontier Science Research Center, University of Miyazaki, 5200 Kihara, Kiyotake, Miyazaki 889-1692, Japan

[2]Organization for Promotion of Tenure Track, University of Miyazaki, Nishi 1-1 Gakuen Kibanadai, Miyazaki, 889-2192, Japan

[3]Cellular and Molecular Biotechnology Research Institute, National Institute of Advanced Industrial Science and Technology (AIST), 2-4-7 Aomi, Koto-ku, Tokyo 135-0064, Japan

[4]Centre to Impact AMR, Monash University, Clayton, VIC 3800, Australia

[5]Infection Program, Biomedicine Discovery Institute, and Department of Microbiology, Monash University, Clayton, VIC 3800, Australia

[6]Department of Materials Science and Engineering, Monash University, Clayton, VIC 3800, Australia

[7]Biomedicine Discovery Institute and Department of Biochemistry and Molecular Biology, Monash University, Clayton 3800, Australia

*e-mail: takuya_shiota@med.miyazaki-u.ac.jp (T.S.), hsin-hui.shen@monash.edu (H.H.S.), trevor.lithgow@monash.edu (T.L.)

ABSTRACT

Outer membrane proteins (OMPs) are essential components of the outer membrane of Gram-negative bacteria. In terms of protein targeting and assembly, the current dogma holds that a "β-signal" imprinted in the final β-strand of the OMP engages the β-barrel assembly machinery (BAM complex) to initiate membrane insertion and assembly of the OMP into the outer membrane. Here, we reveal an additional rule, that signals equivalent to the β-signal are repeated in other, internal β-strands within bacterial OMPs. The internal signal is needed to promote the efficiency of the assembly reaction of these OMPs. BamD, an essential subunit of the BAM complex, recognizes the internal signal and the β-signal, arranging several β-strands for rapid OMP assembly. The internal signal-BamD ordering system is not essential for bacterial viability but is necessary to retain the integrity of the outer membrane against antibiotics and other environmental insults.

TEASER

Bacterial outer membrane proteins are recognized and bound by BamD at specific signals located in multiple β-strands at the C-terminus of these proteins.

MAIN TEXT

INTRODUCTION

In Gram-negative bacteria outer membrane proteins (OMPs) play important roles in membrane-mediated processes (Lundquist et al., 2021; Tommassen, 2010; Walther et al., 2009). Structurally, each major OMP has a β-barrel transmembrane domain, spanning the membrane as a cylindrical structure formed from amphiphilic, antiparallel β-strands (Konovalova et al., 2017; Schulz, 2000). Starting as nascent polypeptides synthesized by ribosomes in the cytoplasm, these newly synthesized OMPs cross the inner membrane in a process mediated by the SecYEG translocon (Manting et al., 2000; Mori and Ito, 2001), and then traverse the periplasm supported by the periplasmic chaperones(Wang et al., 2021). The molecular machine driving OMP insertion and assembly into the membrane is the β-barrel Assembly Machinery complex (BAM complex) (Bakelar et al., 2016; Gu et al., 2016; Iadanza et al., 2016). Given this essential role, and its location on the bacterial cell surface, the BAM complex has emerged as an attractive antibiotic target (Hart et al., 2019; Imai et al., 2019; Kaur et al., 2021; Luther et al., 2019).

In *E. coli*, the BAM complex is composed of five subunits BamA, BamB, BamC, BamD and BamE (Bakelar et al., 2016; Gu et al., 2016; Iadanza et al., 2016; Wu et al., 2005). BamA, the essential core-subunit, is embedded in the outer membrane and projects an extensive N-terminal domain consisting of five polypeptide transport-associated (POTRA) repeats into the periplasm which interacts with other subunits (Noinaj et al., 2013; Voulhoux, 2003). There is some variation in the lipoprotein subunits that are present in the BAM complex varies in different bacterial lineages (Anwari et al., 2012; Webb et al., 2012) but both BamA and the lipoprotein BamD are found in the BAM complexes of all bacterial lineages and are essential for viability in *E. coli* (Malinverni et al., 2006; Webb et al., 2012; Wu et al., 2005). The interaction of the POTRA domains of BamA with its partner BamD contributes to a large, funnel-like feature of the BAM complex which expands into the periplasm.

BamA belongs to Omp85-superfamily protein conserved across bacterial lineages and organelles (Heinz and Lithgow, 2014; Wu et al., 2005). Omp85-superfamily proteins are themselves β-barrels, utilizing a transiently open lateral gate between the first and last

β-strands as the catalytic site of the OMPs assembly (Doyle et al., 2022; Doyle and Bernstein, 2021, 2019; Noinaj et al., 2013; Takeda et al., 2021; Tomasek et al., 2020; Xiao et al., 2021). Biophysical studies have shown "snap-shot" structures of assembly intermediates of the BAM complex with substrate OMPs and demonstrated that during assembly the first strand of the lateral gate of the BamA interacts with the C-terminal strand of the substrate OMPs (Doyle et al., 2022; Shen et al., 2023; Takeda et al., 2023; Tomasek et al., 2020; Wu et al., 2021). OMPs contain a conserved sequence termed the "β-signal" located within this C-terminus strand (Kutik et al., 2008; Paramasivam et al., 2012; Struyvé et al., 1991; Wang et al., 2021). Inhibitory compounds such as darobactin show a similar structure to that of the β-signal and are capable of interacting with the lateral gate (Imai et al., 2019; Kaur et al., 2021; Xiao et al., 2021). The current dogma suggested by these studies dictate that this β-signal should engage directly with the lateral gate in BamA (Horne and Radford, 2022; Tomasek and Kahne, 2021).

Despite recent advances in resolving the BAM complex structure and its function, the molecular mechanism of early stage OMP assembly remains enigmatic. It has been shown that the β-signal plays a significant role in the targeting and folding of BAM complex substrates (Kutik et al., 2008; Wang et al., 2021), yet several important OMPs do not have a recognizable β-signal motif in their C-terminal sequence (Celik et al., 2012; Hagan et al., 2015). For instance, BamA itself lacks an apparent C-terminal β-signal (Hagan et al., 2015). Also, a comprehensive study of the autotransporter class of OMPs, including proteins such as EspP, showed that while 1038 non-redundant proteins did have a C-terminal β-signal motif, over 40% of these proteins had a β-signal motif only in internal strands (Celik et al., 2012), which was also suggested to be the case for BamA (Hagan et al., 2015). It remains to be tested if these internal motifs function as β-signals and how they engage the BAM complex.

Before substrate OMPs can enter the lateral gate of BamA, they must first pass through the periplasmic features of the BAM complex. Although the assembly reactions that occur at the lateral gate are well understood, less is known about the molecular mechanisms at the early stage, prior to being position in the lateral gate. The specific points that have been established are that the substrate makes contact with the BamB and BamD subunits and the lateral gate of the BamA subunit (Hagan et al., 2013; Harrison, 1996; Ieva et al., 2011).

Here, we establish a screening system based on an *in vitro* reconstituted membrane assay using a translocation-competent *E. coli* Microsomal Membrane (EMM) (Gunasinghe et al., 2018; Thewasano et al., 2023) and demonstrate that OMPs - including the major porins that are the predominant substrate of the BAM complex - contain multiple β-signal related repeats. Comparison of the C-terminal β-signal with what we refer to here as the "internal signal", revealed the essential elements of sequence and orientation in the signals that are recognized by the BAM complex. Internal signals and β-signals are recognized by BamD and are responsible for rapid assembly of the OMP into the bacterial membrane at the early stage. Moreover, *in situ* crosslinking and mutagenesis demonstrated that the specific relationship between the BAM complex and this dual signal plays an important role in the integrity of the outer membrane.

RESULTS

Peptidomimetics derived from *E. coli* OmpC inhibit OMP assembly

The EMM assembly assay provides a means for *in vitro* reconstitution of BAM complex function, where the assembly of a ^{35}S-labelled OMP can be monitored (fig. S1A) (Gunasinghe et al., 2018; Thewasano et al., 2023). EspP, a model OMP substrate, belongs to autotransporter family of proteins. Autotransporters have two domains; (1) a β-barrel domain, assembled into the outer membrane via the BAM complex, and (2) a passenger domain, which traverses the outer membrane via the lumen of the β-barrel domain itself and is subsequently cleaved by the correctly assembled β-barrel domain (Celik et al., 2012). When EspP is correctly assembled into outer membrane, a visible decrease in the molecular mass of the protein is observed due to the self-proteolysis. Once the barrel domain is assembled into the membrane it becomes protease-resistant, with residual unassembled and passenger domains degraded (Leyton et al., 2014; Roman-Hernandez et al., 2014). When applied to ^{35}S-labelled EspP, the assay discriminates assembly of a protease-protected β-barrel domain, assembled into the outer membrane by the BAM complex (Ieva et al., 2011), from the protease-sensitive extracellular passenger domain (Fig. 1A) that are degraded by protease (fig. S1B). The addition of peptides with BAM complex affinity, such as the OMP β-signal, are capable of exerting an inhibitory effect by competing for binding of substrate OMPs to the BAM complex (Hagan et al., 2015). Thus, the addition of peptides derived from the entirety of OMPs to the EMM assembly assay, which can evaluate assembly efficiency with high accuracy, expects to identify novel regions that have affinity for the BAM complex. To screen for potential peptidomimetics that could inhibit BAM complex function, a synthetic peptide library was designed for coverage of the sequence features in OmpC (fig. S2). We used peptides that mapped the entirety of OmpC, with a two amino acid overlap. This we considered preferable to peptides that were restricted by structural features, such as β-strands, in consideration that β-strand formation may or may not have occurred in early-stage interactions at the BAM complex.

Six peptides (4, 10, 17, 18, 21, and 23) were found to inhibit EspP assembly (Fig. 1A). Of these, peptide 23 corresponds to the canonical β-signal of OMPs: it is the final β-strand of OmpC and it contains the consensus motif of the β-signal (ζxGxx[Ω/Φ]x[Ω/Φ]). The inhibition seen with peptide 23 indicated that our peptidomimetics screening system using EspP can detect signals recognized by the BAM complex. In addition to inhibiting EspP assembly, five of the most potent peptides (4, 17, 18, 21, and 23) inhibited additional model OMPs; the porins OmpC and OmpF, the peptidoglycan-binding OmpA, and the maltoporin LamB (fig. S3). Comparing the sequences of these inhibitory peptides suggested the presence of a sub-motif from within the β-signal, namely [Ω/Φ]x[Ω/Φ] (Fig. 1B). The sequence codes refer to conserved residues such that: ζ, is any polar residue; G is a glycine residue; Ω is any aromatic residue; Φ is any hydrophobic residue and x is any residue (Hagan et al., 2015; Kutik et al., 2008). The non-inhibitory peptide 9 contained some elements of the β-signal but did not show inhibition of EspP assembly (Fig. 1A).

Peptide 18 also showed a strong sequence similarity to the consensus motif of the β-signal (Fig. 1B) and, like peptide 23, had a strong inhibitory action on EspP assembly (Fig. 1A). Variant peptides based on the peptide 18 sequence were constructed and tested in the EMM assembly assay (Fig. 1C). This analysis revealed that the position 0 (0Φ), in addition to the [Ω/Φ]x[Ω/Φ], motif was functionally important to inhibitory action (Fig.

1C). Thus, we hypothesized the elements of an internal β-signal (hereafter the internal signal) to be Φxxxxx[Ω/Φ]x[Ω/Φ].

Mutations to a putative internal signal results in loss of OMP assembly

To assess the impact of the conserved residues in the potential internal signal for OMP assembly, a series of mutant OmpC variants were constructed and assayed for assembly in the EMM assay (Fig 2A). Three of the peptide regions are present in the final 5 β-strands of OmpC. We denoted these as the first (-1), third (-3), and fifth (-5) β strands from the C-terminus of the barrel. Note, since peptide 17 and peptide 18 overlap, they were considered together as a single region. Given the antiparallel structure of a β-barrel the -1, -3 and -5 strands are orientated in the same direction, and these three strands all conform to the putative Φxxxxx[Ω/Φ]x[Ω/Φ] motif.

BN-PAGE analysis was employed to measure the efficiency of OmpC trimer assembly (Fig. 2A). These gels separate membrane proteins that have been solubilized from native membranes, allowing time-course analysis of protein assembly. Among the mutants with significantly reduced assembly efficiency, Y286A, Y325A, and Y365A correspond to Ω/Φ in position 6 (Ω/Φ), and F280A corresponds to Φ in position 0 of the putative signal (Fig. 2A and fig. S4A). In terms of the highly conserved residues present, sequence conservation was mapped against the β-strands of OMPs whose structures have been determined (fig. S5, S6, and S7). Analysis showed the -5 strand of OmpF and LamB includes residues that conform to the putative Φxxxxx[Ω/Φ]x[Ω/Φ] motif (Fig. 2B). We constructed mutants to the 0Φ or 6[Ω/Φ] positions of the -5 strand in OmpF and LamB, these are the OmpF(V279A), OmpF(Y285A), LamB(V333A) and LamB(Y339A) mutants (Fig. 2B). BN-PAGE analysis showed that both the Φ – OmpF(V279) and LamB(V333) - and Ω/Φ – OmpF(Y285) and LamB(Y339) - residues were important for the assembly of OmpF and LamB (fig. S4B, C).

To address whether the results seen *in vitro* in the EMM assays were consistent with phenotypes drawn from intact *E. coli* cells, we constructed arabinose-inducible plasmids to express mutants of Φ (position 0), the [Ω/Φ] (position 6) and a double mutant combination of both positions in either the -5 or -1 strands of OmpC. To distinguish these plasmid-encoded OmpC variants from the endogenous, chromosome-encoded OmpC, a FLAG epitope tag was incorporated into the region of OmpC immediately behind the cleavage site for the secretory signal sequence (Fig. 3A) (Rapoport, 2007). Expression of FLAG-OmpC variants was induced with 0.1% arabinose, as confirmed through immunoblotting of total cell lysate (Fig. 3B). In comparing the *E. coli* strains, a marked reduction was seen in the steady-state level of the double (“FY” or "VY") mutants OmpC (F280A+Y286A or V359A+Y365A) (Fig. 3C). Little change was evident in the expression levels of the single -1 mutants, suggesting that a fully conserved β-signal located at the C-terminus alone is not essential to maintaining OmpC assembly. To further investigate the nature of the defects, the various strains were analyzed BN-PAGE. In all cases, OmpC that has been detergent-solubilized from outer membranes migrates as a characteristic population of dimeric and trimeric forms under conditions of the BN-PAGE (Fig. 3D). Both the trimeric and dimeric forms of OmpC solubilized from the β-barrel arrays in the outer membrane have equivalent structural and functional properties (Rocque and McGroarty, 1989). The double (“FY” or "VY") mutants displayed drastic reductions of the dimer and trimer (Fig. 3D). As a control, the level and integrity of the BAM complex were monitored and found to be equivalent in all strains (Fig. 3C, and D). Taken

together these results suggest either the internal signal (in strand -5) or the C-terminal β-signal (in strand -1) must be present to achieve efficient assembly of OmpC into the outer membrane.

The internal signal is necessary for insertion step of assembly into OM

The β-signal located in the C-terminal β-strand is important for recognition by the BAM complex. In addition, because it is the last β-strand, it also contributes to engagement with the first β-strand in order that purified OMPs can fold into β-barrels, even in the absence of the BAM complex in artificial non-membrane environments such as detergent micelles (Burgess et al., 2008). To compare this property of strand-engagement for β-barrel folding in detergent micelles, we purified urea-denatured OmpC and the OmpC variant proteins with mutations in the -5 strand (F280A and Y286A) and the -1 strand (V359A and Y365A). The spontaneous folding of each OmpC variant was assessed by the rate of formation of trimer in the presence of detergent micelles (fig.S8A). Trimer embedded into detergent micelles migrated at 100 kDa in this assay system, whereas non-folded monomeric OmpC migrated at 37 kDa (fig. S8). Relative to the rate/extent of trimer formation observed for OmpC(WT), mutations to the [Ω/Φ] (position 6) in the -5 strand i.e. OmpC(Y286A) or the -1 strand i.e. OmpC(Y365A) showed significantly impaired spontaneous folding. Position 6 is an amino acid that contributes to the aromatic girdle. Since Y286A and Y365A affected OMP folding as measured in folding experiments, their positioning into the aromatic girdle may contributes to the efficiency of β-barrel folding, in addition to contributing to the internal signal. Mutation of the Φ residue (position 0) in the -5 strand i.e. OmpC(F280A) or the -1 strand i.e. OmpC(V359A) maintained a similar ability to assemble into micelles as native OmpC. Thus, the conserved features of both -1 and -5 strands have equivalent impact on intrinsic properties for spontaneous folding of β-barrel of OmpC.

We further analyzed the role of internal β-signal by the EMM assembly assay. Compared to the rate at which the trimeric form of OmpC is assembled (Fig. 4A), OmpC(Y286A) is slow and the gels resolve that most of the ^{35}S-labelled OmpC(Y286A) is held in a high-molecular-weight species for most of the time-course. Only at 80 min of assembly has substantial amount of the ^{35}S-labelled OmpC(Y286A) been resolved from this assembly intermediate ("Int") to a native, trimeric form (Fig. 4A). In analyzing assembly intermediates of other sorts of membrane proteins in mitochondria, a version of this analysis referred to as "gel shift" BN-PAGE analysis has been developed (Shiota et al., 2012). Here, the addition of an antibody recognizing the surface-exposed BamC to the samples prior to electrophoresis resulted in a dramatic shift *i.e.* retardation of electrophoretic mobility due to the added mass of antibodies. This is consistent with OmpC(Y286A) being held in an assembly intermediate engaged with the BAM complex (Fig. 4B). Consistent with this, the assembly intermediate which was prominently observed at the OmpC(Y286A) can be extracted from the membranes with urea; urea extraction of the membrane samples prior to analysis by BN-PAGE showed that the integral membrane trimer form of OmpC and OmpC(Y286A) were not extracted by urea (Fig. 4C). Conversely, the assembly intermediate was completely extracted with urea, as expected for a substrate engaged in protein-protein interactions with a proteinaceous complex in the membrane fraction. These results suggest that the mutation in OmpC(Y286A) causes a longer interaction with the BAM complex, as a species of protein that is not yet inserted into the surrounding membrane environment.

Three subunits of the BAM complex have been previously shown to interact with the substrates: BamA, BamB, and BamD (Hagan et al., 2013; Harrison, 1996; Ieva et al., 2011). *In vitro* pull-down assay showed that while BamA and BamD can independently bind to the *in vitro* translated OmpC polypeptide (Fig .S9A), BamB did not (Fig. S9B). To test for signal-dependent binding, BamA and BamD were pre-incubated with inhibitor peptides (Fig. 5A). Peptide 23 inhibited binding of the substrate by BamA and peptide 18 inhibited binding of the substrate by BamD. Peptide 21 inhibited binding of the substrate by either BamA or BamD. These results suggest that BamA and BamD are important for recognition of both the β-signal and the internal signal. While the biochemical assay demonstrated that the OmpC(Y286A) mutant forms a stalled intermediate with the BAM complex, in a state in which membrane insertion was not completed, biochemical assays such as this cannot elucidate where on BamA-BamD this OmpC(Y286A) substrate is stalled. Neutron reflectometry (NR) is a powerful tool for probing the details of substrate-chaperone interactions, and is ideally suited for membrane-embedded proteins (Shen et al., 2014). The rationale to these experiments is that NR provides: (i) information on the distance of specified subunits of a protein complex away from the atomically flat gold surface to which the complex is attached, and (ii) allows the addition of samples between measurements, so that multi-step changes can be made to, for example, detect changes in domain conformation in response to the addition of a substrate. To apply NR imaging to monitor the engagement of OmpC with the BAM complex, BamA was immobilized on an Ni-NTA atomic flat gold-coated silicon wafer to orient the POTRA domain distal to the silicon wafer as previously described (Ding et al., 2020). A lipid layer was reconstituted to provide BamA with a membrane-like environment prior to sequential measurement of: (i) BamA with lipid (1st measurement), (ii) BamA with lipid and BamD (2nd measurement), and (iii) BamA-BamD-lipid with the addition of OmpC (WT) or OmpC(Y286A) (3rd measurement) (fig. S10A).

Comparing the reflectivity profiles of three measurements (Fig. 5B), changes were observed in the layers after the addition of BamD and OmpC(Y286A), as seen in a shift of fringe to low Q range around 0.02-0.03 $Å^{-1}$. Crystal structures show that the periplasmic domains of BamA can be treated as two rigid bodies: POTRA1-POTRA2(P1-2) and POTRA3-POTRA4-POTRA5(P3-5). Thus, for further data analysis, we analyzed BamA as four layers: the His6 extra-cellular layer where BamA is attached to the chip, the membrane layer (containing the β-barrel domain of BamA), an adjoining P3-5 layer, and the N-terminal P1-2 layer. NR data can then highlight variations in thickness of these layers, which corresponds to the position of additional protein mass in each point of measurement (Fig. 5C, fig. S10B, C).

On addition of BamD (2nd measurement), the scattering length density (SLD) profiles showed that BamD was located in the P3-5 layer (Fig. 5C, fig. S10D, E), an observation consistent with previous studies on the resting BAM complex (Ding et al., 2020). On addition of the OmpC(Y286A) substrate (3rd measurement) binding was observed to the P3-5 layer, with a concomitant extension of this layer from 29.7±0.8 Å to 45.5±1.6 Å away from the membrane (Fig. 5C, 5D, fig. S10F,G). By contrast, no obvious changes were observed on the addition of the native OmpC protein implying that interactions it makes with BamA or BamD on the Si-Wafer were resolved too quickly to capture (fig. S11). The failure to observe changes with the WT-OmpC control in the NR analysis is consistent with the data from the BN-PAGE analysis (Fig. 4A) where native OmpC does not form the stable intermediate seen for OmpC(Y286A). The NR findings indicate that OmpC(Y286A) is stacked at a position in the BAM complex with the

POTRA3-5 of BamA and BamD, and that the Y286A mutation results in a relatively stable binding to this specific periplasmic region of the BAM complex.

BamD acts as a receptor for the internal signal and β-signal

To elucidate the residues within BamD that mediate this signal-receptor interaction, we applied *in vitro* site-specific photo-crosslinking (fig. S12A). A library of 40 BamD variants was created to incorporate the non-natural amino acid, *p*-benzoyl-$_L$-phenylalanine (BPA), by the suppressor tRNA method in a series of positions (Chin et al., 2002). We purified 40 different BPA variants of BamD, and then irradiated UV after incubating with ^{35}S-labelled OmpC. The UV-dependent appearance of crosslinks between OmpC and BamD occurred for 17 of the BamD variants (fig. S12B). Structurally, these amino acids locate both the lumen side of funnel-like structure (e.g. 49 or 62) and outside of funnel-like structure such as BamC binding site (e.g. 114) (fig. S12C). The analysis was repeated to determine BamD cross-links for ^{35}S-labelled OmpC(WT), the internal signal mutant OmpC(Y286A), or the β-signal mutant OmpC(βAAA: Y365A, Q366A, F367A) (fig. S12D). This mapping of OmpC binding showed that an N-terminal section of BamD (amino acid residues 60 or 65) interacts with the internal signal, while a distinct section of BamD (amino acid residues 196, 200, 204) interacts with β-signal (fig. S12E).

While *in vitro* site-specific photo-crosslinking provides information on the substrate receptor region of BamD, this data only indirectly measures which residues of OmpC are being recognized. As our peptidomimetic screen identified conserved features in the internal signal, and cross-linking highlighted the N-terminal and C-terminal TPR motifs of BamD as regions of interaction with OmpC, we focused on amino acids specifically within the β-signals of OmpC and regions of BamD which interact with β-signal. We purified a form of BamD that is substituted with a cysteine residue in the substrate-binding region, and synthesized forms of ^{35}S-labeled OmpC substituted with a cysteine residue at various positions. Treatment with 1 μM $CuSO_4$ can stimulate disulfide formation between BamD and OmpC (Fig. 6A). Consistent with the BPA crosslinking data, the positions near the internal signal in OmpC (amino acid residues 278, 284, 296 and 302) formed disulfide bonds with the N-terminal section of BamD (amino acid residues 49, 65). Conversely, residues towards the C-terminal, canonical β-signal of OmpC (amino acid residues 333, 357, and 363) formed disulfide bonds with a C-terminal section of BamD (at amino acid residue 204) (Fig. 6B). All of disulfide crosslinked products were validated by reducing condition SDS-PAGE (fig. S13).

To further probe this interaction, we engineered an *E. coli* strain to expressed BPA-containing BamD and a FLAG-tagged form of OmpC and performed *in vivo* photo-crosslinking (Fig. 6C). These western blots reveal cross-linked products representing the interacting protein species. Photo cross-linking of unnatural amino acid is not a 100% efficient process, so the level of cross-linked products is only a small proportion of the molecules interacting in the assays. In BamD, BPA at positions 49, 53, 65, or 196 generated cross-links to FLAG-OmpC. Positions 114 and 200 in BamD were not detected to interact with OmpC. Positions 49, 53, 65, and 196 of BamD face the interior of the funnel-like structure of the periplasmic domain of the BAM complex, while position 114 is located outside of the funnel-like structure (Bakelar et al., 2016; Gu et al., 2016; Iadanza et al., 2016). We note that while position 114 was cross-linked with OmpC *in vitro* using purified BamD, that this was not seen with *in vivo* cross-linking. Instead, in the context of the BAM complex, position 114 of BamD binds to the BamC subunit and would not be

available for substrate binding *in vivo* (Bakelar et al., 2016; Gu et al., 2016; Iadanza et al., 2016).

Two structurally distinct regions of BamD promote OmpC folding and assembly

In order to directly measure how the β-strands of OmpC come together, we established a new assay in which the folding of purified OmpC can be measured with or without assistance by purified BamD. Using the crystal structure of OmpC as a guide, cysteine residues were engineered in place of amino acids that were outward-facing on the final five β-strands of folded OmpC, placed close enough to a cysteine residue in the adjacent β-strand to allow for the possibility of disulfide formation once the strands had been correctly aligned in the folded protein (Fig. 7A). These cysteine-variant OmpC proteins were incubated with or without BamD to determine how efficiently disulfide bonds formed. Samples harboring cysteine residues in OmpC that were incubated with BamD migrated faster than non-Cys OmpC on non-reducing SDS-PAGE (Fig. 7B). This migration difference was not observed in reducing conditions, validating that the faster migration occurred as a result of internal molecule disulfide bond formation. Disulfide bonds were formed in each of the paired strands β-strands from -1 to -5, suggesting that BamD directly stimulates arrangement of C-terminal five strands of BamD.

Cross-linking studies shown in Fig 6B indicated 2 distinct regions of BamD as hot-spots for OmpC-binding. Anticipating that binding sites would be conserved; we analyzed sequence conservations and found BamD(Y62) and BamD(R197) as good candidates proximal to OmpC binding sites (Fig. 7C). R197 has previously been isolated as a suppressor mutation of a BamA temperature sensitive strain (Ricci et al., 2012). Each residue was located on the lumen side of the funnel-like structure in the EspP-BAM assembly intermediate structure (PDBID; 7TTC) (Doyle et al., 2022). Mutant strains expressing BamD(Y62A) and BamD(R197A) in a genetic background where the chromosomal bamD can be depleted by an arabinose-responsive promoter were tested (Fig. 7D and fig. S14A,B,C). Growth conditions were established wherein we could deplete endogenous BamD but not disturb cell growth (fig. S14D, fig. S15A). Isolated EMM from this time point showed that neither the BamD(Y62A) nor the BamD(R197A) mutants affected the steady-state protein levels of other components of the BAM complex (fig. S15B), nor did they impact the complex formation of the BAM complex (Fig. 7E, fig. S15C). The EMM assembly assay showed that the internal signal binding site was as important as the β-signal binding site to the overall assembly rates observed for OmpC (Fig. 7F), OmpF (fig. S15D), and LamB (fig. S15E). These results suggest that recognition of both the C-terminal β-signal and the internal signal by BamD is important for efficient protein assembly.

BamD is responsible for OMP assembly to retain outer membrane integrity

In *E. coli*, BamD function is essential for cell viability (Onufryk et al., 2005). As a result, in an *E. coli* strain where bamD expression is under the control of an arabinose-inducible promoter, in a control strain (Fig. 8A, “vec”) two rounds of dilution in restrictive growth media depletes the level of BamD protein and stops cell growth (Fig. 8A). The BamD(Y62A) mutant and the BamD(R197A) mutant supported viability (Fig. 8A, fig. S15A), allowing membrane fractions to be isolated from each mutant strain: the steady-state level of porins OmpA and OmpC/OmpF was reduced in the BamD(Y62A) and BamD(R197A) mutants (Fig. 8B). This was also true when the level of trimeric OmpF was

assessed by native PAGE: less OmpF trimer had been assembled over the growth period relative to the steady-state level of the BAM complex (Fig. 8C). Thus, while these mutant forms of BamD support cell viability (Fig. 8A), they have deleterious effects on β-barrel protein assembly *in vivo*. In the case of the BamD(Y62A) strain, growth in the presence of vancomycin showed impaired outer membrane integrity (Fig. 8D,8E).

Vancomycin sensitivity is a classic assay to measure membrane integrity in Gram-negative bacteria such as *E. coli* because the drug vancomycin cannot permeate the outer membrane except if outer membrane integrity is breached by any means. Then, and only then, is sensitivity to vancomycin seen (Hart and Silhavy, 2020). To test whether expression of a mutant form of OmpC that cannot engage BamD *in vivo* would likewise diminish membrane integrity, we assayed for growth of *E. coli* strains expressing OmpC(FY) and other mutant forms of OmpC (Fig. 8F, 8G). The OmpC(FY) -5 strand double mutant showed increased sensitivity to vancomycin (Fig. 8G). The OmpC(FY) mutant does not accumulate in the outer membrane to the level found in wild-type *E. coli* (Fig. 3D). The strain co-expressing OmpC(FY) with endogenous OmpC has diminished levels of another major porin (OmpF) as judged by BN-PAGE, but not OmpC(WT) (Fig. 8I, see also Fig. 3). The dimeric form of endogenous OmpF was prominently observed in both the OmpC(WT) as well as the OmpC(VY) double mutant cells.

DISCUSSION

OMPs are the major components of bacterial outer membranes, accounting for more than 50% of the mass of the outer membrane (Horne et al., 2020; Jarosławski et al., 2009). The quantitative analysis of single-cell data suggests approximately 500 molecules of major porins, such as OmpC or OmpF, are assembled into the outer membrane per minute per cell (Benn et al., 2021; Lithgow et al., 2023). This considerable task requires factors that promote the efficient and prompt assembly of OMPs in order to handle this extraordinary rate of substrate protein flux. The efficiency of assembly is necessary to fight against external cellular insult, hence the use of BamD as an OMP assembly accelerator.

In our experimental approach to assess for inhibitory peptides, specific segments of the major porin substrate OmpC were shown to interact with the BAM complex as peptidomimetic inhibitors. Results for this experimental approach went beyond expected outcomes by identifying the essential elements of the signal Φxxxxxx[Ω/Φ]x[Ω/Φ] in β-strands other than the C-terminal strand. Discovery of conserved, internal signals in OMPs explains two previous reports where the -5 strand of BamA was suggested to be more similar to a β-signal motif than the C-terminal strand of BamA (Hagan et al., 2013; Imai et al., 2011) and a hidden Markov model analysis that showed that in autotransporter OMPs, a class of OMPs which includes EspP, 473/1511 of non-redundant proteins show no β-signal motif at the C-terminal strand, but instead containrd a β-signal motif in the -5 strand (Celik et al., 2012; Cox et al., 2010).

The inhibitory peptides discovered here contained information that led us to define an internal signal for OMP assembly. This internal signal corresponds to the -5 strand in OmpC and is recognized by BamD. Sequence analysis shows that similar sequence signatures are present in other OMPs (Figs. S5, S6 and S7). These sequences were investigated in two further OMPs: OmpF and LamB (Fig. 2C and D). Hidden Markov model approaches like HMMR (Eddy, 1995) detect conserved sequence features and tools such as MEME (Bailey et al., 2009) can then define a sequence motif derived from information across very many non-redundant protein sequences. The abundance of information which arises from modeling approaches and from the multitude of candidate OMPs, is generally oversimplified when written as a primary structure description typical of the β-signal for bacterial OMPs (i.e. ζxGxx[Ω/Φ]x[Ω/Φ]) (Kutik et al., 2008). Analysis of the few peptidomimetic peptide sequences in functional analyses, via both *in vitro* assays and intact *E. coli* analysis, suggests that Φxxxxx[Ω/Φ]x[Ω/Φ] is a descriptor for the internal signal, which is complimentary in function to the C-terminal β-signal that engages the BAM complex to assist OMP assembly into the outer membrane.

The β-signal motif (ζxGxx[Ω/Φ]x[Ω/Φ]) is an eight-residue consensus, and internal signal motif is composed of a nine-residue consensus. Recent structures have shown the lateral gate of BamA interacts with a 7-residue span of substrate OMPs. Interestingly, inhibitory compounds, such as darobactin, mimic only three resides of the C-terminal side of β-signal motif. Cross-linking presented here in our study showed that BamD residues R49 and G65 cross-linked to the positions 0 and 6 of the internal signal in OmpC (Fig. 6D). Both signals are larger than the assembly machineries signal binding pocket, implying that the signal might sit beyond the bounds of the signal binding pocket in BamD and the lateral gate in BamA. These finding are consistent with similar observations in other signal sequence recognition events, such as the mitochondrial targeting presequence

signal that is longer than the receptor groove formed by the Tom20, the subunit of the translocator of outer membrane (TOM) complex (Yamamoto et al., 2011). The presequence has been shown to bind to Tom20 in several different conformations within the receptor groove (Nyirenda et al., 2013).

The current dogma in our field states that the information contained in the β-signal is important for engagement into the lateral gate of BamA (Bitto and McKay, 2003; de Cock et al., 1997; Doyle et al., 2022; Doyle and Bernstein, 2019; Hagan et al., 2015; Jansen et al., 2000; Robert et al., 2006; Tomasek et al., 2020; Xiao et al., 2021). This interaction initiates the insertion of a nascent OMP polypeptide into the outer membrane. By this model, BamD is considered to function by organizing the BamC and BamE subunits of the BAM complex against the core subunit BamA (Kim et al., 2011, 2007; Malinverni et al., 2006). If that is the sole role of BamD, then BamD is essential because its importance in structural organization of the BAM complex (Hart and Silhavy, 2020), not because of a substrate recognition function. Previous studies have shown BamD is capable of stimulating the folding and insertion of OMPs into liposomes in the absence of BamA (Hagan et al., 2013, 2010). The question remains, how is BamD capable of this function? In our present study, we show that incubation of OmpC with BamD promotes the formation of antiparallel β-strands by the formation of intra-molecular disulfide cross-linking of neighboring β-strands at the C-terminus (Fig. 7B). In EspP position 1214, located within the internal signal, was seen to cross-link to BamD (Ieva et al., 2011), and our inter-molecular cysteine cross-linking showed the N-terminal helices of BamD's TPR structure interacts with the internal signal and the C-terminal helices interacts with the β-signal (Fig. 6B, C). Failure in this interaction was seen to stall substrate assembly within the soluble domain of the BAM complex (Fig 4C and 5D). This suggests that BamD acts in an important role in an early recognition step in which both the substrate's C-terminal β-signal and internal signal engage BamD in order to be arranged into a form ready for transfer to the lateral gate of BamA (Shen et al., 2023; Tomasek et al., 2020) (Fig 9A). This adds an additional role of the C-terminus of BamD beyond a complex stability role (Ricci et al., 2012; Storek et al., 2023). The recognition and initiation of β-strand formation by BamD is necessary to support the efficient assembly of the 500 molecules of OMPs per minute required by the outer membrane, ensuring the survival against foreign insult and supports bacterial survival (Lithgow et al., 2023).

Recent advances in our understanding of BAM complex function have come from structural determination of EspP engaged in assembly by the BAM complex (Doyle et al., 2022; Shen et al., 2023). The assembly intermediate of EspP engaged with the BAM complex shows the -4 strand, interacts with the R49 residue of BamD, in the N-terminal substrate binding region, even before the -5 strand had entered into this cavity (Doyle et al., 2022). Spatially, this indicates the BamD can serve to organize two distinct parts of the nascent OMP substrate at the periplasmic face of the BAM complex, either prior to or in concert with, engagement to the lateral gate of BamA. Assessing this structurally showed the N-terminal region of BamD (interacting with the POTRA1-2 region of BamA) and the C-terminal region of BamD (interacting with POTRA5 proximal to the lateral gate of BamA) (Bakelar et al., 2016; Gu et al., 2016; Tomasek et al., 2020) has the N-terminal region of BamD changing conformation depending on the folding states of the last four β-strands of the substrate OMP, EspP (Doyle et al., 2022). The overall effect of this being a change in the dimensions of this cavity change, a change which is dependent on the folded state of the substrate engaged in it (Fig 9 B-E). We showed that purified BamD can facilitate partial folding of an OMP and we propose that BamD captures the -1 strand and draws the -5 strand by a conformational change, thereby catalyzing the formation of

hydrogen bonds to form β-hairpins in neighboring strands, to prime the substrate for insertion into the outer membrane by the action of BamA. After OMP assembly, all elements of the internal signal are positioned such that they face into the lipid-phase of the membrane. This observation may be a coincidence, or may be utilized by the BAM complex to register and orientate the lipid facing amino acids in the assembling OMP away from the formative lumen of the OMP. Amino acids at position 6, such as Y286 in OmpC, are not only component of the internal signal for binding by the BAM complex, but also act in structural capacity to register the aromatic girdle for optimal stability of the OMP in the membrane.

MATERIALS AND METHODS

E. coli strains and Growth conditions

E. coli strains used in this study are listed in Table S1. All strains were grown in LB (1% tryptone, 1% NaCl, and 0.5% yeast extract). *E. coli* strains used for the *in vivo* photo-crosslinking experiments were grown in XB (1% tryptone, 1% NaCl, and 0.1% yeast extract). Unless otherwise specified, ampicillin (amp; 50 mg/ml), chloramphenicol (Cm; 10 mg/ml), or kanamycin (Kan, 30 mg/ml) were added to media for plasmid selection.

To create the BamD-depletion strain, we amplified four DNA fragments encoding 540 to 40 base pairs of the 5´ UTR of BamD (primers BamDSO-1 and -2), kanamycin cassette (primers BamDSO-3 and -4), AraC-pBAD (primers BamDSO-5 and -6), and the first 500 bp of BamD (primers BamSO-7 and -8), respectively (Figure S16). Table S2 describes the pair of primers and template DNA to amplify each DNA fragment. These four DNA fragments were combined by the overlap PCR method and transformed into MC4100a harboring pKD46 encoding λ Red recombinase (Datsenko and Wanner, 2000). Transformants were selected in the presence of kanamycin and 0.1% (w/v) $_L$-arabinose.

To culture BamD-depletion strains a single colony from each BamD-depletion strains harboring pBamD variants was inoculated into LB (+ amp + Kan + 0.02% (w/v) $_L$-arabinose) and cultured for 10 h at 37°C. The saturation culture was shifted into the LB (+ amp + Kan) and incubated for another 10h at 37°C. The saturation culture was diluted into LB (+ amp + kan + 0.5% (w/v) $_D$-Glucose) to an OD_{600} = 0.02, and incubated at 37°C until cell density reached OD_{600}=0.8. A second dilution in the same media to an OD_{600} = 0.02 was performed, and incubated for 2.5h at 37°C.

Plasmids

Plasmids and primers used in this study are listed in Tables S3 to S7. Cloning of specific target gene ORFs into specified vectors was performed via SLiCE *in vitro* recombination (Okegawa and Motohashi, 2015).

Protein Purification

Plasmids encoding each subunit of the BAM complex and OmpC genes (including a His_6-tag) were transformed into BL21(DE3)* cells (Invitrogen). BamD and OmpC variant transformants were grown in LB (+ amp) at 37°C to an OD_{600} = 0.5. Expression was induced by adding 1 mM IPTG and the cells grown at 37°C for 3 h. For BamD containing BPA mutations, MC4100 cells were transformed with pHIS-BamD-(X)-amber and pEVOL-BpF45. Transformants were cultured in LB with antibiotics to an OD_{600} = 0.5, then supplemented with 1 mM BPA, 0.05% (w/v) $_L$-arabinose and 1 mM IPTG to induce expression. Cells were grown at 37°C for a further 3 h.

Cells were pelleted by centrifugation at 6,000 x *g* for 10 min. Pellets were resuspended in Buffer A (150 mM NaCl, 20 mM $NaPO_4$) and lysed via sonication. Lysates were clarified by low-speed centrifugation of 1100 x *g* for 10 min at 4°C. For purification of BamD variant proteins, supernatants were again clarified by high-speed centrifugation, 17000 x *g* for 15 min at 4°C. High-speed clarified supernatants were then applied Ni_2+-NTA-affinity column chromatography. Ni_2+-NTA resin were washed by Buffer A with 50 mM imidazole and proteins were eluted in Buffer A containing an imidazole step gradient (100 - 400 mM). Peak fractions were collected as the purified fraction. To purify OmpC, the pellets containing OmpC in inclusion bodies were resuspended in Buffer A containing 0.5% Triton X-100 and centrifuged for 11,600 x *g* for 10 min at 4°C. Inclusion bodies were denatured in Buffer A with 6 M urea and mixed at 25°C for 90 min, followed by centrifugation of 11,600 x *g* for 10 min at 4°C. The filtered

supernatant was applied to Ni_2+-NTA-affinity column chromatography. The bound OmpC-His_6 was washed with Buffer A (+ 6 M urea, 50 mM imidazole) and eluted with Buffer A containing 6M urea and 200 mM imidazole. Purified proteins were then diluted with glycerol (final concentration of 10%), snap frozen in liquid nitrogen and stored in -80°C. BamA was purified as detailed previously (Ding et al., 2020).

Isolation of the *E.coli* microsomal membrane fraction (EMM)

E. coli crude membrane fraction were isolated as previously described (Gunasinghe et al., 2018). In brief, pelleted cells were resuspended in sonication buffer (50 mM Tris-HCl pH 7.5, 150 mM NaCl, 5 mM EDTA) and lysed via sonication on ice. After low-speed centrifugation (1,100 x *g*, 5 min, 4°C), supernatant was centrifuged again (15,000 x *g*, 10 min, 4°C). Pelleted membranes were resuspended in SEM buffer (250 mM sucrose, 10 mM MOPS-KOH pH 7.2, 1 mM EDTA) and flash frozen. Protein concentrations of EMM were calculated by OD_{280} measurements of 100 times diluted in 0.6% SDS (OD_{280}=0.21 was set to be 10 mg/ml).

EMM assembly assay

The EMM assembly assay has been previously described (Gunasinghe et al., 2018; Thewasano et al., 2023). The method in brief is as follows; substrates were prepared via *in vitro* transcription by SP6-RNA polymerase followed by *in vitro* translation in rabbit reticulocyte lysate supplemented with ^{35}S-methionine. EMMs were resuspended in Assembly Assay buffer (10 mM MOPS-KOH pH7.2, 2.5 mM KH2PO4, 250 mM sucrose, 15 mM KCl, 5 mM MgCl2, 2 mM methionine, 5 mM DTT, 1% w/v BSA, 0.09% v/v Triton X-100), and incubated with ^{35}S-labelled substrate at 30°C for indicated time points. Assembly reactions were halted by moving to ice for 5 minutes. The EMMs were then harvested via centrifugation at 15,0000 x *g* for 5 min at 4°C and washed with SEM buffer. After SEM buffer wash, trimeric protein assembled EMM pellets were solubilized in 1.5% DDM containing Blue native (BN)-PAGE Lysis Buffer (25 mM imidazole-HCl pH 7.0, 50 mM NaCl, 50 mM 6-aminohexanoic acid, 1 mM EDTA, 7.5% (w/v) glycerol) on ice for 20 minutes. Solubilized proteins were clarified by centrifugation of 15,000 x *g* for 10 min at 4°C, followed by BN-PAGE analysis as described previously (Gunasinghe et al., 2018; Thewasano et al., 2023).

Peptide library was synthesized by MIMOTOPES, and resuspended in DMSO at a concentration of 30 mM. The peptide inhibition screen of EspP was performed as stated above, but with the addition of 0.1 mM inhibitory peptide to the Assembly Assay buffer and incubated with EMMs for 5 minutes prior to the addition of ^{35}S-labelled substrate protein. After harvesting, EMMs were treated with 100 µg/mL Proteinase K on ice for 20 minutes. Digestion was halted by adding 2 mM PMSF. The EMMs were then collected via centrifugation at 15,0000 x *g* for 5 min at 4°C and washed with SEM buffer. EspP assembled with EMM proteins were analyzed by SDS-PAGE and radio-imaging. EMM assembly of trimeric proteins was tested with the addition of 0.25 mM peptide and analyzed as above.

Sequence conservation analysis

For conservation analysis, we obtained homologous sequences of representative structure-known beta barrel outer membrane proteins from reference bacterial proteomes in UniProt (The UniProt Consortium, 2019) using phmmer and jackhammer HMMER 3.2.1 (http://hmmer.org). The best hit sequences in organisms which also contained a BamD homolog were used. We identified 31, 94, 25, 19, 27, 44, 43, 23, 42, 22, 132, 46,

58, 68, 39, 245, 261,115, 187, 250 and 74 sequences for OmpA, OmpW, PagP, OmpX, OmpT, EspP, Hbp, NanC, OMPLA, Tsx, FadL, OmpC, OmpF, PhoE, LamB, BtuB, Cir, FecA, FepA, FhuA and PapC, respectively (sequence identity less than 60%, expect for OmpX. In case of OmpX, sequence identity is less than 80% due to the small number of sequences). Multiple alignments were generated by MAFFT (Katoh et al., 2019) and then sequence logos of -5th transmembrane strands were created using WebLogo 3 (Crooks, 2004).

In vivo assembly analysis of FLAG-OmpC

We introduced a FLAG epitope tag into the N-terminal region of OmpC, immediately behind the cleavage site for the SEC-signal sequence (Rapoport, 2007), to distinguish between endogenous OmpC and the OmpC variants in the OmpC-deletion strain background which has issues of diminished OM integrity. The expression of FLAG-OmpC mutants was controlled by using a plasmid-based pBADara promoter cassette, to avoid the chronic effect of constitutively expressed mutant proteins (Figure 3A). We transformed pBAD-FLOmpC variants into MC4100A. Transformants were cultured in LB (+ amp) until OD600=0.5 and then protein expression induced by adding 0.1% arabinose for 3 h. *E. col*i cells were harvested and total cell lysate or EMMs prepared accordingly.

Antibody Shift Assay

The variation of BN-PAGE analysis referred to as an antibody shift assay was performed as previously described with modification (Shiota et al., 2012). In brief, solubilized EMMs were incubated with 3 μL of anti-BamC antibodies for 45 min at 4°C. Samples were clarified via centrifugation at 13,000 x *g* for 10 minutes at 4°C, and subjected to BN-PAGE.

Urea Extraction of Intermediate

Once the Assembly Assay was performed, to obtain intermediate complexes, lysates were washed with SEM, the EMMs resuspended in SEM containing 6 M urea and incubated at 37°C for 1 hour, after which 50 mM Tris HCL pH 8.0 was added. Membrane fractions were collected via high-speed centrifugation (100,000 x *g*, 45 min, 25°C) and washed twice with SEM buffer. The membrane was solubilized for 20 minutes at 4°C in 1.5% DDM containing BN-PAGE lysis buffer and subjected to BN-PAGE analysis.

Neutron Reflectometry

Neutron reflection (NR) was carried out on the SOFIA reflectometer at the Materials and Life Science Experimental Facility (MLF) at J-PARC, Japan (Mitamura et al., 2013; Yamada et al., 2011). The reflectivity at the interface between the Si substrate and water solution was measured at 3 incident angles (0.3°, 0.75° and 1.8°). The neutrons were introduced from the substrate side to illuminate the interface and the reflection intensity was normalized by the transmission intensity through the substrate to achieve the reflectivity with the Q range of up to 0.2 Å-1. Neutron reflectivity, denoted as R, is the ratio of the incoming to the exiting neutron beams. It's calculated based on the Momentum transfer Q, which is defined by the formula $Q=4\pi \sin\theta/\lambda$, where θ represents the angle of incidence and λ stands for the neutron wavelength. The approximate value of R(Q) can be expressed as $R(Q)=16\pi^2/ Q^2 |\rho(Q)|^2$, where R(Q) is the one-dimensional Fourier transform of $\rho(z)$, which is the scattering length density (SLD) distribution perpendicular to the surface. SLD is calculated by dividing the sum of the coherent neutron scattering lengths of all atoms in a sample layer by the volume of that layer. Consequently, factors such as

thickness, volume fraction, and interface roughness of the samples significantly influence the intensity of the reflected beams.

Analysis of the NR profiles was performed using the MOTOFIT analysis software (Nelson, 2010). The software uses a conventional method, optical matrix method (Nelson, 2006) to model the reflectivity profiles. Briefly, the layer is divided into several sublayers and then a characteristic matrix is evaluated for each sublayer, from which the whole reflectivity can be calculated exactly. The same layer with multiple datasets with three different isotopic contrasts is fitted simultaneously until the satisfactory fit is obtained (smallest χ^2 value in the genetic algorithm). All models include a 15 Å oxide layer on the surface of the silicon substrates and subsequently there are three layers of Ni, gold and Ni-NTA on the top of oxide layer. Protein layers will assemble outwards from the Ni-NTA layer.

The best-fit model from MOTOFIT gives information about the thickness, density and roughness of each layer. When a layer is composed of just two components, a chemical species or its fragment s and water w, the SLD is given by: where ρw and ρs are the scattering length densities of the two components, respectively and φ is the volume fraction of species s in the layer. If more than one chemical species is present, then ρs is determined by the volume fraction of each species in the layer.

OmpC *in vitro* folding

Urea denatured OmpC and OmpC variants were purified as stated above. Protein was resuspended in Refolding Buffer (10 mM Phosphate Buffer pH 8.0, 2 mM EDTA, 1 mM glycine) to a final concentration of 5 µM. DDM was added to a final concentration of 3.4 mM. Samples were incubated at 37°C for 0, 1, 3, 6, 8, 12, 24, and 36 hours. SDS-Loading dye was added and each sample was split into two tubes (one to be boiled, one at RT for 10min). OmpC folding was analyzed via SDS-PAGE.

Ni-NTA Substrate Pull-down

Purified BamA or BamD was resuspended in Buffer A to a final concentration of 10 µM. Specific peptides or DMSO alone was added (final concentration 0.35 mM) and incubated rocking at 4°C for 1 hour. To each tube, 0.5 µL of ^{35}S-OmpC was added and vortexed vigorously, 10% of the total volume was removed to assay as “input” for each sample. Samples were then incubated at 4°C with rocking for 30 minutes. Ni-NTA agarose beads were add to each sample, incubated at 4°C with rocking for an additional 30 minutes then washed with Buffer A containing 20 mM imidazole. BAM proteins were eluted from the Ni-NTA resin using Buffer A with 400 mM imidazole. Proteins were TCA precipitated and subjected to analysis by SDS-PAGE and imaged via radio-imaging.

Disulfide cross-linking

BamD-OmpC cysteine crosslinking was performed using 50 µM purified single-cysteine BamD mutant variants incubated with 8 µL of single-cysteine OmpC variants translated by the retic in 30 µL of Buffer A at 25°C for 2 min. An oxidizing reaction mixture of 1 µM CuSO4, 4 mM methionine, and 4 mM cysteine was added and incubated at 25°C for 5 min. Proteins were precipitated by TCA precipitation. e and solubilized in 1% SDS buffer. Solubilized proteins were diluted by 0.5% TritonX-100 buffer and purified with Ni-NTA via the tagged BamD-H6. BamD and disulfide crosslink products were eluted with 400 mM imidazole containing 0.5% TritonX-100 buffer. Eluted proteins were concentrated by TCA precipitation and solubilized with SDS-PAGE loading dye with or without β-Me.

The OmpC intrachain disulfide bond assay was performed using 1 μL ^{35}S-OmpC double cysteine variants translated in the presence of 1 mM DTT. OmpC variants were diluted in into 100 μL Buffer A then incubated with 50 μM BamD at 32°C for 30 minutes. 10 μM CuSO4 was added to samples and incubated for an additional 2 minutes, followed by the addition of SDS-PAGE loading dye with or without 5mM DTT and 1% β-Me. Proteins were resolved via SDS-PAGE and imaged as stated above.

In vivo and *in vitro* photo-crosslinking

For *in vivo* photo-crosslinking, MC4100 strain was transformed with pEVOL-pBpF, pTnT-BamAp-BamD-His8, and pET-FLAG-OmpC, with respective antibiotics. A single colony was used to inoculate a culture in photo-crosslinking media (1% NaCl, 1% Tryptone, 0.1% Extract yeast dried, 1mM BPA) for 3 hours at 37°C in the dark. Afterward, arabinose (0.1% final concentration) was added and further incubated for 2.5 h. Cultures were divided with one half UV-irradiated for 7 min at RT and the other half not. Cells were pelleted and solubilized with 1% SDS buffer (50mM Tris-HCl pH 8.0, 150mM NaCl, 1% SDS). His-tagged BamD containing BPA and its cross-linked products were purified by Ni-NTA agarose. Cross-linked products were identified via immunoblotting with anti-BamD and anti-FLAG antibodies.

In vitro photo-crosslinking was performed with 32 μg of purified BamD-His_8 variants containing BPA diluted in Buffer A. 40 μL of ^{35}S-OmpC was added to each tube and incubated at 25°C for 10 minutes in the dark. Each mixture was transferred to the lid of a microtube and irradiated with UV using B-100AP (UVP) for 7 min on ice. 10% (w/v) SDS solution was added to a final concentration of 1%, then incubated at 95°C for 10 min to denature proteins. Protein mixtures were diluted with 0.5% TritonX-100 buffer (50 mM Tris-HCl pH 7.0, 150 mM NaCl, 0.5% Triton-X100), and purified on Ni-NTA agarose beads. Elute fractions were concentrated by TCA precipitation and analyzed by SDS-PAGE and radio-imaging.

Statistical analysis

For all densitometry measurements we utilized “imagequant” quant (ImageQuant TL, cytiva) and statistical analysis and graphing was performed with Microsoft Excel software.

REFERENCES AND NOTES

Anwari K, Webb CT, Poggio S, Perry AJ, Belousoff M, Celik N, Ramm G, Lovering A, Sockett RE, Smit J, Jacobs Wagner C, Lithgow T. 2012. The evolution of new lipoprotein subunits of the bacterial outer membrane BAM complex. *Mol Microbiol* **84**:832–844. doi:10.1111/j.1365-2958.2012.08059.x

Bailey TL, Boden M, Buske FA, Frith M, Grant CE, Clementi L, Ren J, Li WW, Noble WS. 2009. MEME SUITE: tools for motif discovery and searching. *Nucleic Acids Research* **37**:W202–W208. doi:10.1093/nar/gkp335

Bakelar J, Buchanan SK, Noinaj N. 2016. The structure of the β-barrel assembly machinery complex. *Science* **351**:180–186. doi:10.1126/science.aad3460

Benn G, Mikheyeva IV, Inns PG, Forster JC, Ojkic N, Bortolini C, Ryadnov MG, Kleanthous C, Silhavy TJ, Hoogenboom BW. 2021. Phase separation in the outer membrane of *Escherichia coli*. *Proc Natl Acad Sci USA* **118**:e2112237118. doi:10.1073/pnas.2112237118

Bitto E, McKay DB. 2003. The periplasmic molecular chaperone protein SurA binds a peptide motif that is characteristic of integral outer membrane proteins. *J Biol Chem* **278**:49316–49322. doi:10.1074/jbc.M308853200

Burgess NK, Dao TP, Stanley AM, Fleming KG. 2008. Beta-barrel proteins that reside in the *Escherichia coli* outer membrane *in vivo* demonstrate varied folding behavior *in vitro*. *J Biol Chem* **283**:26748–26758. doi:10.1074/jbc.M802754200

Celik N, Webb CT, Leyton DL, Holt KE, Heinz E, Gorrell R, Kwok T, Naderer T, Strugnell RA, Speed TP, Teasdale RD, Likić VA, Lithgow T. 2012. A bioinformatic strategy for the detection, classification and analysis of bacterial autotransporters. *PLoS One* **7**:e43245. doi:10.1371/journal.pone.0043245

Chin JW, Martin AB, King DS, Wang L, Schultz PG. 2002. Addition of a photocrosslinking amino acid to the genetic code of *Escherichia coli*. *Proc Natl Acad Sci USA* **99**:11020–11024. doi:10.1073/pnas.172226299

Cox DL, Luthra A, Dunham-Ems S, Desrosiers DC, Salazar JC, Caimano MJ, Radolf JD. 2010. Surface immunolabeling and consensus computational framework to identify candidate rare outer membrane proteins of Treponema pallidum. *Infect Immun* **78**:5178–5194. doi:10.1128/IAI.00834-10

Crooks GE. 2004. WebLogo: A Sequence Logo Generator. *Genome Research* **14**:1188–1190. doi:10.1101/gr.849004

Datsenko KA, Wanner BL. 2000. One-step inactivation of chromosomal genes in *Escherichia coli* K-12 using PCR products. *Proc Natl Acad Sci USA* **97**:6640–6645. doi:10.1073/pnas.120163297

de Cock H, Struyvé M, Kleerebezem M, van der Krift T, Tommassen J. 1997. Role of the carboxy-terminal phenylalanine in the biogenesis of outer membrane protein PhoE of *Escherichia coli* K-12. *J Mol Biol* **269**:473–478. doi:10.1006/jmbi.1997.1069

Ding Y, Shiota T, Le Brun AP, Dunstan RA, Wang B, Hsu H-Y, Lithgow T, Shen H-H. 2020. Characterization of BamA reconstituted into a solid-supported lipid bilayer as a platform for measuring dynamics during substrate protein assembly into the membrane. *Biochimica et Biophysica Acta (BBA) - Biomembranes* **1862**:183317. doi:10.1016/j.bbamem.2020.183317

Doyle MT, Bernstein HD. 2021. BamA forms a translocation channel for polypeptide export across the bacterial outer membrane. *Molecular Cell* **81**:2000-2012.e3. doi:10.1016/j.molcel.2021.02.023

Doyle MT, Bernstein HD. 2019. Bacterial outer membrane proteins assemble via asymmetric interactions with the BamA β-barrel. *Nat Commun* **10**:3358. doi:10.1038/s41467-019-11230-9

Doyle MT, Jimah JR, Dowdy T, Ohlemacher SI, Larion M, Hinshaw JE, Bernstein HD. 2022. Cryo-EM structures reveal multiple stages of bacterial outer membrane protein folding. *Cell* **185**:1143-1156.e13. doi:10.1016/j.cell.2022.02.016

Eddy SR. 1995. Multiple alignment using hidden Markov models. *Proc Int Conf Intell Syst Mol Biol* **3**:114–120.

Gu Y, Li H, Dong H, Zeng Y, Zhang Z, Paterson NG, Stansfeld PJ, Wang Z, Zhang Y, Wang W, Dong C. 2016. Structural basis of outer membrane protein insertion by the BAM complex. *Nature* **531**:64–69. doi:10.1038/nature17199

Gunasinghe SD, Shiota T, Stubenrauch CJ, Schulze KE, Webb CT, Fulcher AJ, Dunstan RA, Hay ID, Naderer T, Whelan DR, Bell TDM, Elgass KD, Strugnell RA, Lithgow T. 2018. The WD40 protein BamB mediates coupling of BAM complexes into assembly precincts in the bacterial outer membrane. *Cell Rep* **23**:2782–2794. doi:10.1016/j.celrep.2018.04.093

Hagan CL, Kim S, Kahne D. 2010. Reconstitution of outer membrane protein assembly from purified components. *Science* **328**:890–892. doi:10.1126/science.1188919

Hagan CL, Westwood DB, Kahne D. 2013. bam Lipoproteins Assemble BamA in vitro. *Biochemistry* **52**:6108–6113. doi:10.1021/bi400865z

Hagan CL, Wzorek JS, Kahne D. 2015. Inhibition of the β-barrel assembly machine by a peptide that binds BamD. *Proc Natl Acad Sci USA* **112**:2011–2016. doi:10.1073/pnas.1415955112

Harrison SC. 1996. Peptide–Surface Association: The Case of PDZ and PTB Domains. *Cell* **86**:341–343. doi:10.1016/S0092-8674(00)80105-1

Hart EM, Mitchell AM, Konovalova A, Grabowicz M, Sheng J, Han X, Rodriguez-Rivera FP, Schwaid AG, Malinverni JC, Balibar CJ, Bodea S, Si Q, Wang H, Homsher MF, Painter RE, Ogawa AK, Sutterlin H, Roemer T, Black TA, Rothman DM, Walker SS, Silhavy TJ. 2019. A small-molecule inhibitor of BamA impervious to efflux and the outer membrane permeability barrier. *Proc Natl Acad Sci USA* **116**:21748–21757. doi:10.1073/pnas.1912345116

Hart EM, Silhavy TJ. 2020. Functions of the BamBCDE Lipoproteins Revealed by Bypass Mutations in BamA. *J Bacteriol* **202**:e00401-20. doi:10.1128/JB.00401-20

Heinz E, Lithgow T. 2014. A comprehensive analysis of the Omp85/TpsB protein superfamily structural diversity, taxonomic occurrence, and evolution. *Front Microbiol* **5**:370. doi:10.3389/fmicb.2014.00370

Horne JE, Brockwell DJ, Radford SE. 2020. Role of the lipid bilayer in outer membrane protein folding in Gram-negative bacteria. *Journal of Biological Chemistry* **295**:10340–10367. doi:10.1074/jbc.REV120.011473

Horne JE, Radford SE. 2022. Roll out the barrel! Outer membrane tension resolves an unexpected folding intermediate. *Cell* S0092-8674(22)00261–6. doi:10.1016/j.cell.2022.03.001

Iadanza MG, Higgins AJ, Schiffrin B, Calabrese AN, Brockwell DJ, Ashcroft AE, Radford SE, Ranson NA. 2016. Lateral opening in the intact β-barrel assembly machinery captured by cryo-EM. *Nat Commun* **7**:12865. doi:10.1038/ncomms12865

Ieva R, Tian P, Peterson JH, Bernstein HD. 2011. Sequential and spatially restricted interactions of assembly factors with an autotransporter domain. *Proc Natl Acad Sci USA* **108**:E383–E391. doi:10.1073/pnas.1103827108

Imai K, Fujita N, Gromiha MM, Horton P. 2011. Eukaryote-wide sequence analysis of mitochondrial β-barrel outer membrane proteins. *BMC Genomics* **12**:79. doi:10.1186/1471-2164-12-79

Imai Y, Meyer KJ, Iinishi A, Favre-Godal Q, Green R, Manuse S, Caboni M, Mori M, Niles S, Ghiglieri M, Honrao C, Ma X, Guo JJ, Makriyannis A, Linares-Otoya L, Böhringer N, Wuisan ZG, Kaur H, Wu R, Mateus A, Typas A, Savitski MM, Espinoza JL, O'Rourke A, Nelson KE, Hiller S, Noinaj N, Schäberle TF, D'Onofrio A, Lewis K. 2019. A new antibiotic selectively kills Gram-negative pathogens. *Nature* **576**:459–464. doi:10.1038/s41586-019-1791-1

Jansen C, Heutink M, Tommassen J, de Cock H. 2000. The assembly pathway of outer membrane protein PhoE of Escherichia coli. *Eur J Biochem* **267**:3792–3800. doi:10.1046/j.1432-1327.2000.01417.x

Jarosławski S, Duquesne K, Sturgis JN, Scheuring S. 2009. High-resolution architecture of the outer membrane of the Gram-negative bacteria Roseobacter denitrificans. *Mol Microbiol* **74**:1211–1222. doi:10.1111/j.1365-2958.2009.06926.x

Katoh K, Rozewicki J, Yamada KD. 2019. MAFFT online service: multiple sequence alignment, interactive sequence choice and visualization. *Briefings in Bioinformatics* **20**:1160–1166. doi:10.1093/bib/bbx108

Kaur H, Jakob RP, Marzinek JK, Green R, Imai Y, Bolla JR, Agustoni E, Robinson CV, Bond PJ, Lewis K, Maier T, Hiller S. 2021. The antibiotic darobactin mimics a β-strand to inhibit outer membrane insertase. *Nature* **593**:125–129. doi:10.1038/s41586-021-03455-w

Kim KH, Aulakh S, Paetzel M. 2011. Crystal Structure of β-Barrel Assembly Machinery BamCD Protein Complex. *Journal of Biological Chemistry* **286**:39116–39121. doi:10.1074/jbc.M111.298166

Kim S, Malinverni JC, Sliz P, Silhavy TJ, Harrison SC, Kahne D. 2007. Structure and function of an essential component of the outer membrane protein assembly machine. *Science* **317**:961–964. doi:10.1126/science.1143993

Konovalova A, Kahne DE, Silhavy TJ. 2017. Outer Membrane Biogenesis. *Annu Rev Microbiol* **71**:539–556. doi:10.1146/annurev-micro-090816-093754

Kutik S, Stojanovski D, Becker L, Becker T, Meinecke M, Krüger V, Prinz C, Meisinger C, Guiard B, Wagner R, Pfanner N, Wiedemann N. 2008. Dissecting Membrane Insertion of Mitochondrial β-Barrel Proteins. *Cell* **132**:1011–1024. doi:10.1016/j.cell.2008.01.028

Leyton DL, Johnson MD, Thapa R, Huysmans GHM, Dunstan RA, Celik N, Shen H-H, Loo D, Belousoff MJ, Purcell AW, Henderson IR, Beddoe T, Rossjohn J, Martin LL, Strugnell RA, Lithgow T. 2014. A mortise–tenon joint in the transmembrane domain modulates autotransporter assembly into bacterial outer membranes. *Nat Commun* **5**:4239. doi:10.1038/ncomms5239

Lithgow T, Stubenrauch CJ, Stumpf MPH. 2023. Surveying membrane landscapes: a new look at the bacterial cell surface. *Nat Rev Microbiol*. doi:10.1038/s41579-023-00862-w

Lundquist K, Billings E, Bi M, Wellnitz J, Noinaj N. 2021. The assembly of β-barrel membrane proteins by BAM and SAM. *Mol Microbiol* **115**:425–435. doi:10.1111/mmi.14666

Luther A, Urfer M, Zahn M, Müller M, Wang S-Y, Mondal M, Vitale A, Hartmann J-B, Sharpe T, Monte FL, Kocherla H, Cline E, Pessi G, Rath P, Modaresi SM, Chiquet P, Stiegeler S, Verbree C, Remus T, Schmitt M, Kolopp C, Westwood M-A, Desjonquères N, Brabet E, Hell S, LePoupon K, Vermeulen A, Jaisson R, Rithié V, Upert G, Lederer A, Zbinden P, Wach A, Moehle K, Zerbe K, Locher HH, Bernardini F, Dale GE, Eberl L, Wollscheid B, Hiller S, Robinson JA, Obrecht D. 2019. Chimeric peptidomimetic antibiotics against Gram-negative bacteria. *Nature* **576**:452–458. doi:10.1038/s41586-019-1665-6

Malinverni JC, Werner J, Kim S, Sklar JG, Kahne D, Misra R, Silhavy TJ. 2006. YfiO stabilizes the YaeT complex and is essential for outer membrane protein assembly in *Escherichia coli*: YfiO assembles OMPs and stabilizes the YaeT complex. *Molecular Microbiology* **61**:151–164. doi:10.1111/j.1365-2958.2006.05211.x

Manting EH, van Der Does C, Remigy H, Engel A, Driessen AJ. 2000. SecYEG assembles into a tetramer to form the active protein translocation channel. *EMBO J* **19**:852–861. doi:10.1093/emboj/19.5.852

Mitamura K, Yamada NL, Sagehashi H, Torikai N, Arita H, Terada M, Kobayashi M, Sato S, Seto H, Goko S, Furusaka M, Oda T, Hino M, Jinnai H, Takahara A. 2013. Novel neutron reflectometer SOFIA at J-PARC/MLF for in-situ soft-interface characterization. *Polym J* **45**:100–108. doi:10.1038/pj.2012.156

Mori H, Ito K. 2001. The Sec protein-translocation pathway. *Trends Microbiol* **9**:494–500. doi:10.1016/s0966-842x(01)02174-6

Nelson A. 2010. *Motofit* – integrating neutron reflectometry acquisition, reduction and analysis into one, easy to use, package. *J Phys: Conf Ser* **251**:012094. doi:10.1088/1742-6596/251/1/012094

Nelson A. 2006. Co-refinement of multiple-contrast neutron/X-ray reflectivity data using *MOTOFIT*. *J Appl Crystallogr* **39**:273–276. doi:10.1107/S0021889806005073

Noinaj N, Kuszak AJ, Gumbart JC, Lukacik P, Chang H, Easley NC, Lithgow T, Buchanan SK. 2013. Structural insight into the biogenesis of β-barrel membrane proteins. *Nature* **501**:385–390. doi:10.1038/nature12521

Nyirenda J, Matsumoto S, Saitoh T, Maita N, Noda NN, Inagaki F, Kohda D. 2013. Crystallographic and NMR evidence for flexibility in oligosaccharyltransferases and its catalytic significance. *Structure* **21**:32–41. doi:10.1016/j.str.2012.10.011

Okegawa Y, Motohashi K. 2015. A simple and ultra-low cost homemade seamless ligation cloning extract (SLiCE) as an alternative to a commercially available seamless DNA cloning kit. *Biochemistry and Biophysics Reports* **4**:148–151. doi:10.1016/j.bbrep.2015.09.005

Onufryk C, Crouch M-L, Fang FC, Gross CA. 2005. Characterization of six lipoproteins in the sigmaE regulon. *J Bacteriol* **187**:4552–4561. doi:10.1128/JB.187.13.4552-4561.2005

Paramasivam N, Habeck M, Linke D. 2012. Is the C-terminal insertional signal in Gram-negative bacterial outer membrane proteins species-specific or not? *BMC Genomics* **13**:510. doi:10.1186/1471-2164-13-510

Rapoport TA. 2007. Protein translocation across the eukaryotic endoplasmic reticulum and bacterial plasma membranes. *Nature* **450**:663–669. doi:10.1038/nature06384

Ricci DP, Hagan CL, Kahne D, Silhavy TJ. 2012. Activation of the *Escherichia coli* β-barrel assembly machine (Bam) is required for essential components to interact properly with substrate. *Proc Natl Acad Sci U S A* **109**:3487–3491. doi:10.1073/pnas.1201362109

Robert V, Volokhina EB, Senf F, Bos MP, Van Gelder P, Tommassen J. 2006. Assembly factor Omp85 recognizes its outer membrane protein substrates by a species-specific C-terminal motif. *PLoS Biol* **4**:e377. doi:10.1371/journal.pbio.0040377

Rocque WJ, McGroarty EJ. 1989. Isolation and preliminary characterization of wild-type OmpC porin dimers from Escherichia coli K-12. *Biochemistry* **28**:3738–3743. doi:10.1021/bi00435a017

Roman-Hernandez G, Peterson JH, Bernstein HD. 2014. Reconstitution of bacterial autotransporter assembly using purified components. *eLife* **3**. doi:10.7554/eLife.04234

Schulz GE. 2000. β-Barrel membrane proteins. *Current Opinion in Structural Biology* **10**:443–447. doi:10.1016/S0959-440X(00)00120-2

Shen C, Chang S, Luo Q, Chan KC, Zhang Z, Luo B, Xie T, Lu G, Zhu X, Wei X, Dong C, Zhou R, Zhang X, Tang X, Dong H. 2023. Structural basis of BAM-mediated outer membrane β-barrel protein assembly. *Nature*. doi:10.1038/s41586-023-05988-8

Shen H-H, Leyton DL, Shiota T, Belousoff MJ, Noinaj N, Lu J, Holt SA, Tan K, Selkrig J, Webb CT, Buchanan SK, Martin LL, Lithgow T. 2014. Reconstitution of a nanomachine driving the assembly of proteins into bacterial outer membranes. *Nature Communications* **5**. doi:10.1038/ncomms6078

Shiota T, Maruyama M, Miura M, Tamura Y, Yamano K, Esaki M, Endo T. 2012. The Tom40 assembly process probed using the attachment of different intramitochondrial sorting signals. *MBoC* **23**:3936–3947. doi:10.1091/mbc.e12-03-0202

Storek KM, Sun D, Rutherford ST. 2023. Inhibitors targeting BamA in gram-negative bacteria. *Biochim Biophys Acta Mol Cell Res* 119609. doi:10.1016/j.bbamcr.2023.119609

Struyvé M, Moons M, Tommassen J. 1991. Carboxy-terminal phenylalanine is essential for the correct assembly of a bacterial outer membrane protein. *J Mol Biol* **218**:141–148. doi:10.1016/0022-2836(91)90880-f

Takeda H, Busto JV, Lindau C, Tsutsumi A, Tomii K, Imai K, Yamamori Y, Hirokawa T, Motono C, Ganesan I, Wenz L-S, Becker T, Kikkawa M, Pfanner N, Wiedemann N, Endo T. 2023. A multipoint guidance mechanism for β-barrel folding on the SAM complex. *Nat Struct Mol Biol* **30**:176–187. doi:10.1038/s41594-022-00897-2

Takeda H, Tsutsumi A, Nishizawa T, Lindau C, Busto JV, Wenz L-S, Ellenrieder L, Imai K, Straub SP, Mossmann W, Qiu J, Yamamori Y, Tomii K, Suzuki J, Murata T, Ogasawara S, Nureki O, Becker T, Pfanner N, Wiedemann N, Kikkawa M, Endo T. 2021. Mitochondrial sorting and assembly machinery operates by β-barrel switching. *Nature* **590**:163–169. doi:10.1038/s41586-020-03113-7

Thewasano N, Germany EM, Maruno Y, Nakajima Y. 2023. Categorization of *Escherichia coli* Outer Membrane Proteins by Dependence on Accessory Proteins of the β-barrel Assembly Machinery Complex. *J Biol Chem* **in press**. doi:10.1016/j.jbc.2023.104821

Tomasek D, Kahne D. 2021. The assembly of β-barrel outer membrane proteins. *Current Opinion in Microbiology* **60**:16–23. doi:10.1016/j.mib.2021.01.009

Tomasek D, Rawson S, Lee J, Wzorek JS, Harrison SC, Li Z, Kahne D. 2020. Structure of a nascent membrane protein as it folds on the BAM complex. *Nature* **583**:473–478. doi:10.1038/s41586-020-2370-1

Tommassen J. 2010. Assembly of outer-membrane proteins in bacteria and mitochondria. *Microbiology (Reading)* **156**:2587–2596. doi:10.1099/mic.0.042689-0

Voulhoux R. 2003. Role of a Highly Conserved Bacterial Protein in Outer Membrane Protein Assembly. *Science* **299**:262–265. doi:10.1126/science.1078973

Walther DM, Rapaport D, Tommassen J. 2009. Biogenesis of β-barrel membrane proteins in bacteria and eukaryotes: evolutionary conservation and divergence. *Cell Mol Life Sci* **66**:2789–2804. doi:10.1007/s00018-009-0029-z

Wang X, Peterson JH, Bernstein HD. 2021. Bacterial Outer Membrane Proteins Are Targeted to the Bam Complex by Two Parallel Mechanisms. *mBio* **12**. doi:10.1128/mBio.00597-21

Webb CT, Heinz E, Lithgow T. 2012. Evolution of the β-barrel assembly machinery. *Trends Microbiol* **20**:612–620. doi:10.1016/j.tim.2012.08.006

Wu R, Bakelar JW, Lundquist K, Zhang Z, Kuo KM, Ryoo D, Pang YT, Sun C, White T, Klose T, Jiang W, Gumbart JC, Noinaj N. 2021. Plasticity within the barrel domain of BamA mediates a hybrid-barrel mechanism by BAM. *Nat Commun* **12**:7131. doi:10.1038/s41467-021-27449-4

Wu T, Malinverni J, Ruiz N, Kim S, Silhavy TJ, Kahne D. 2005. Identification of a multicomponent complex required for outer membrane biogenesis in *Escherichia coli*. *Cell* **121**:235–245. doi:10.1016/j.cell.2005.02.015

Xiao L, Han L, Li B, Zhang M, Zhou H, Luo Q, Zhang X, Huang Y. 2021. Structures of the β□barrel assembly machine recognizing outer membrane protein substrates. *FASEB j* **35**. doi:10.1096/fj.202001443RR

Yamada NL, Torikai N, Mitamura K, Sagehashi H, Sato S, Seto H, Sugita T, Goko S, Furusaka M, Oda T, Hino M, Fujiwara T, Takahashi H, Takahara A. 2011. Design and performance of horizontal-type neutron reflectometer SOFIA at J-PARC/MLF. *Eur Phys J Plus* **126**:108. doi:10.1140/epjp/i2011-11108-7

Yamamoto H, Itoh N, Kawano S, Yatsukawa Y, Momose T, Makio T, Matsunaga M, Yokota M, Esaki M, Shodai T, Kohda D, Hobbs AEA, Jensen RE, Endo T. 2011. Dual role of the receptor Tom20 in specificity and efficiency of protein import into mitochondria. *Proc Natl Acad Sci U S A* **108**:91–96. doi:10.1073/pnas.1014918108

Acknowledgments

We thank the members of the Shiota, Shen and Lithgow labs for discussion and critical comments on the manuscript. This work was supported by JSPS KAKENHI to TS (19K16077, 18KK0197, 18H06052, 22K12672 and 21KK0126), to EMG (21K15043), and to KI (18K11543 and 21H03551), JST FOREST Program to TS (JPMJFR2064), AMED Research Support Project for Life Science and Drug Discovery (Basis for Supporting Innovative Drug Discovery and Life Science Research (BINDS)) (23ama121029j0002) to KI, Australian Research Council (DP160100227) to TL, and National Health and Medical Research Council (CDF1106798) to HHS. The following grants are also acknowledged; a grant from the Ichiro Kanehara Foundation for the Promotion of Medical Sciences and Medical Care, Waksman Foundation of Japan, Tokyo Biochemical Research Foundation, Sumitomo Foundation, Naito Foundation, Uehara Memorial Foundation, The Shinnihon Foundation of Advanced Medical Treatment Research, and Noguchi institute (to TS) and National Health and Medical Research Council (2016330) to TL. The NR experiment at the J-PARC MLF was performed under a user program (Proposal No. 2019B0364). We thank NL Yamada for support of NR measurements, and H. Nishitoh for access to instruments (for TS). Radiation experiments were supported by the RI Kiyotake of the Frontier Science Research Center, University of Miyazaki.

Competing interests: Authors declare that they have no competing interests.

Data and materials availability: All data are available in the main text or the supplementary materials.

SUPPLEMENTARY MATERIALS

This PDF file includes
Legends for Supplementary figures.
Figs. S1 to S16
Tables S1 to S7
References for Supplementary materials

FIGURE LEGENDS

Fig. 1 | Peptides derived from β-strands of OmpC selectively inhibit OMP assembly. **A and C**, ^{35}S-labelled EspP was synthesized by rabbit reticulocyte lysate, then incubated with EMM, and samples prepared for analysis by SDS-PAGE and radio-imaging (see Methods). EspP assembly into EMM was performed in the presence of DMSO (D) or specific inhibitor peptides. The precursor (p) and mature (m) form of EspP are indicated. **A**, Peptides labelled 1 through 23 were derived from OmpC, while peptide 24 was taken from a mitochondrial β-barrel protein to serve as a negative control (see fig. S2). **B,** Sequence comparison of inhibitor peptides identified in the EspP assembly assays. The signal is comprised of key hydrophobic (Φ), polar (ζ), glycine (G), and 2 aromatic (Ω) or hydrophobic amino acids. Amino acids highlighted in blue conform to the consensus signal, while those highlighted in purple deviate from the consensus signal. **C**, Upper: sequence of the peptide 18 indicating residue codes for the mutated peptides e.g. at position "6", the native residue Y was mutated to A in peptide "6A". Position 0 designates the first hydrophobic residue and position 8 designates the final aromatic or hydrophobic residue. DMSO (D) was used for control. Middle: SDS-PAGE of EspP assembly assay. Lower: data for inhibition of EspP assembly into EMM assayed in the presence of each of the indicated peptides.

Fig. 2 | Mutations in β-signals inhibit OMP Assembly *in vitro*.
A, Representation of OmpC, (upper panel) annotated to show the position of each b-strand (blue arrows) and the region mimicked in the indicated peptides. Sequence logos show the conservation of sequence for the residues in these regions (see Methods), where the height of letter corresponds to the degree of conservation across bacterial species, residues are color-coded: aromatic (orange), hydrophobic (green), basic (blue), acidic (red), polar (sky blue) and proline and glycine (black). In the lower panel, data from the EMM assembly assay of OmpC mutants is organized to show effects for key mutants: ^{35}S-labelled OmpC wild-type or mutant proteins were incubated with EMM for 30 or 90 min, and analyzed by BN-PAGE and radio-imaging. B, Comparison of amino acids in the final and 5th to final (-5) β-strands of OmpC, OmpF, and LamB. All three OMPs contain the putative hydrophobic residue near the N-terminal region of the β-strands, highlight with a black box. A hydrophobic and an aromatic residue is also found to be highly conserved between these OMP β-strands at the C-terminal amino acids of the β-strands. C-D, Assembly of ^{35}S-labelled OmpF (C) or LamB (D) with mutations to the -5 β-strand or final β-strand in to EMM. Samples were prepared as in A.

Fig. 3 | Modifications in the putative internal signal slow the rate of OMP assembly *in vivo*.
A, Schematic model of FLAG-OmpC expression system in *E. coli*. The plasmid-borne copy of OmpC was mutated and the mutant proteins are selectively detected with antibodies to the FLAG epitope. **B,** Total cell lysates were prepared from the variant *E. coli* strains expressing FLAG-OmpC (WT), -5 strand mutants: F280A, Y286A, double mutant F280A/Y286A (FY), or final β-strand mutants: V359A, Y365A, double mutant V359A/Y365A (VY) with (+) or without (-) arabinose. The steady-state levels of the indicated proteins were assessed after SDS-PAGE by immunoblotting with anti-FLAG antibody. **C**, After growth with arabinose induction, EMM fraction was isolated from each of the FLAG-OmpC variant expressing *E. coli* strains to assess steady state levels of OmpC variants and BAM complex subunits: BamA, BamB, BamC, BamD, and BamE by SDS-PAGE and immunoblotting. **D**, EMM fractions were solubilized with 1.5% DDM and

subjected to BN-PAGE and immunoblotting. The indicated proteins were detected by anti-FLAG (top) and anti-BamA antibodies (bottom), respectively.

Fig. 4 | Mutation that stalls OMP assembly in a high molecular weight assembly intermediate.

A, Upper panel, assembly assay of ^{35}S-OmpC wild-type (WT) and mutant Y286A. After incubation in the EMM assays for indicated time points, ^{35}S-proteins were resolved via BN-PAGE. OmpC trimer and intermediate (int) are indicated. The lower panel shows a quantification of the intermediate form compared to total assembled protein (average of 3 independent experiments). Statistical significance was indicated by the following: N.S. (not significant), $p<0.05$; *, $p<0.005$; **. Exact p values of intermediate formed by Wt vs Y286A at each timepoint were as follows; 20 minutes: $p = 0.03077$, 40 minutes: $p = 0.02402$, 60 minutes: $p = 0.00181$, 80 minutes: $p = 0.0545$. **B,** ^{35}S-labelled OmpC(Y286A) was incubated with EMM for 60 mins, then the EMM fraction was solubilized with 1.5% DDM and incubated with (+) or without (-) anti-BamC antibody for 40 min. These samples were then analyzed by BN-PAGE. The presumptive translocation intermediate (Int) and the gel-shift species (Int. +AB) are indicated. **C,** ^{35}S-labelled OmpC was incubated with EMM and then analyzed by BN-PAGE and radio-imaging. EMM were then washed and solubilized in the presence (+) or absence (-) of 6 M urea, after which the membrane fraction was re-isolated via ultracentrifugation for 45 min. Isolated membranes were solubilized in 1.5% DDM and analyzed by BN-PAGE.

Fig. 5 | Proximity and dependence of BamD with OmpC(Y286A) revealed by Neutron Reflectometry analysis.

A, Ni-NTA was used to affinity purify His6-BamA or His6-BamD. The protein-Ni-NTA bead complex were then incubated in the presence of DMSO or the indicated peptides resuspended in DMSO, and ^{35}S-labelled OmpC was incubated with these beads. After washing, bound proteins were eluted with 400 mM imidazole buffer. The graph represents densitometry analysis of data from 3 independent experiments. **B,** NR profiles for BamA in membrane (1st measurement, square black line), after addition of BamD (2nd measurement, circle red line), and after addition of the OmpC(Y286A) substrate (3rd measurement, triangle blue line). The experimental data was fitted using a seven-layer model: chromium - gold - NTA - His_8 - β-barrel - P3-5 - P1-2. **C,** Table summarizes of the thickness, roughness and volume fraction data of each layer from the NR analysis. The thickness refers to the depth of layered structures being studied as measured in Å. The roughness refers to the irregularities in the surface of the layered structures being studied as measured in Å. 1st, 2nd, and 3rd measurement displayed in black, magenta, and blue, respectively. P3-5: POTRA3, POTRA 4, and POTRA5, P1-2: POTRA1 and POTRA2, Lipid: POPC, Solution: D_2O, gold match water (GMW) and H_2O. Details were described in Table S8 to S10. **D**, Neutron reflectometry schematic of BamA (green), BamD (yellow) and OmpC(Y286A) (magenta). Numbers indicate corresponding POTRA domains of BamA. Note that the cartoon is a depiction of the results and not a scale drawing of the structures.

Fig. 6 | BamD acts as the receptor for internal β-signals.

A, BamD-cys mutant proteins were purified and incubated with ^{35}S-OmpC with cysteine mutations from the -5 to the final β-strand. After the addition of the oxidizing agent, $CuSO_4$, samples were purified with Ni-NTA and analyzed by SDS-PAGE. **B,** BamD cysteine mutants, highlighted in magenta, formed disulfide bonds at distinct locations of

OmpC. **C,** BPA containing BamD was expressed in the presence (+) or absence (-) of FLAG-OmpC overexpression. Pink arrows indicate BamD-FLAG-OmpC cross-link products. **D,** OMP substrate superimposed on BamD. BamD cross-linking positions corresponding to internal signal are marked in purple and substrate cross-linking regions are marked in orange.

Fig. 7 | Key residues in two structurally distinct regions of BamD promote β-strand formation and OMP assembly.
A, Double cysteine residues were mutated into OmpC between anti-parallel β-strands to form artificial disulfide bonds **B**,^{35}S-OmpC-cys variants were translated then incubated with (+) or without (-) BamD. The samples were analyzed by reducing or non-reducing condition. Disulfide bond specific bands (S-S) are indicated to the right of the gel. **C,** Sequence conservation analysis of BamD. Target residues, Y62 and R197, are indicated with dark pink spheres on the crystal structure of BamD, sequence logos represent conservation in the immediate region of these residues. Amino acids listed above logo sequence are from crystal structure. Sequence conservation of BamD (bottom). **D**, Schematic depiction of the BamD depletion strain of *E. coli* used to express mutant BamD proteins. **E**, Pull-down assay of the variants of BamD-His8. The EMMs as in **(C)** were solubilized with 1.5% DDM and then subjected to Ni-NTA. T- 5% total input, F- unbound fraction, W- wash fraction, E- Eluted fraction. Each fraction was analyzed by SDS-PAGE and immunoblotting against indicated antibodies. **F**, Assembly of OmpC was reduced in EMMs containing BamD mutated at Y62 and R197. ^{35}S-labelled OmpC was incubated with EMM as in (**C**), and then analyzed by BN-PAGE and radio-imaging.

Fig. 8 | Substrate recognition by BamD is essential to maintain membrane integrity.
A, Strains of *E. coli* with a depletion of chromosomal *bamD*, complemented by expression of the indicated forms of BamD, were grown in restrictive media (LB supplemented with 0.5% glucose) for 4 hours, then diluted into fresh media and grown a further 4 hours, then diluted into fresh media and grown a further 4 hours. **B,** Quantitation of steady-state protein levels of OmpF and the indicated subunits of the BAM complex in WT, Y62A, R197A mutants were determined after SDS-PAGE and immunoblot analysis. Wedge indicates that in each case, two samples were assessed corresponding to either 4 μg or 12 μg of total protein. **C**, Quantitation of the level of trimeric OmpF formed in the indicated EMM assays. The immunoblot analysis is shown after BN-PAGE analysis and immunoblotting with antibodies recognizing OmpF (upper panel) or BamD (lower panel). **D, E** *E coli* bamD depletion cells expressing mutations at residues, Y62A and R197A, in the β-signal recognition regions of BamD were grown with of VCN. **F, G,** *E coli* cells expressing mutations to OmpC internal signal, as shown in Fig 3, grown in the presence of VCN. Mutations to two key residues of the internal signal were sensitive to the presence of VCN. **H**, Structure of BamD (top) and the final 5 β-strands of OmpC (bottom). Gray boxes indicate relative regions of interaction between BamD and substrates. **I**, OmpF complex assembly *in vivo* of cells expressing mutant OmpC. OmpF assembly was greatly reduced in cells expressing double mutations to the -5 internal β-signal.

Fig. 9| Model for the recognition of internal and canonical β-signals by the BAM complex.
A, BAM complex assisted-OMP assembly is initiated when substrate OMPs encounter the periplasmic domain of the BAM complex. The canonical β-signal (blue arrow) of the OMP engages with the C-terminal TPR motifs of BamD (pink), after which the internal β-signal (orange arrow) is marshalled by the N-terminal TPR motif. The internal signal

interacts with BamD R49 and N60 (black stars) while the canonical β-signal interacts with BamD D204 (black star). The proximity of BamD-substrate to POTRA 5 and the organization of the C-terminal β-strands of OMPs can then stimulate the entrance to the lateral gate of BamA. Finally, barrel formation and release into the membrane follows as previously published28,29. **B,** Structure of substrate engaged BAM complex (PDBID: 6V05). **C,** Bottom-up view of periplasmic domain of complex as shown in (B). Arrows indicate the position of the residues on BamD that function in binding sites for -5 signal and the β signal. **D,** A cavity formed by POTRA 1-2 and POTRA 5 of BamA and BamD is sufficient to accommodate the C-terminal five β-strands of substrate OMP. Substrate -1 strand and -5 β-strand are indicated by light blue strand and orange strand, respectively. The signal binding region of BamD is emphasized by deep purple (PDBID; Bam complex: 7TT5 and 7TT2). **E,** Bottom-up view of complex as shown in (D).

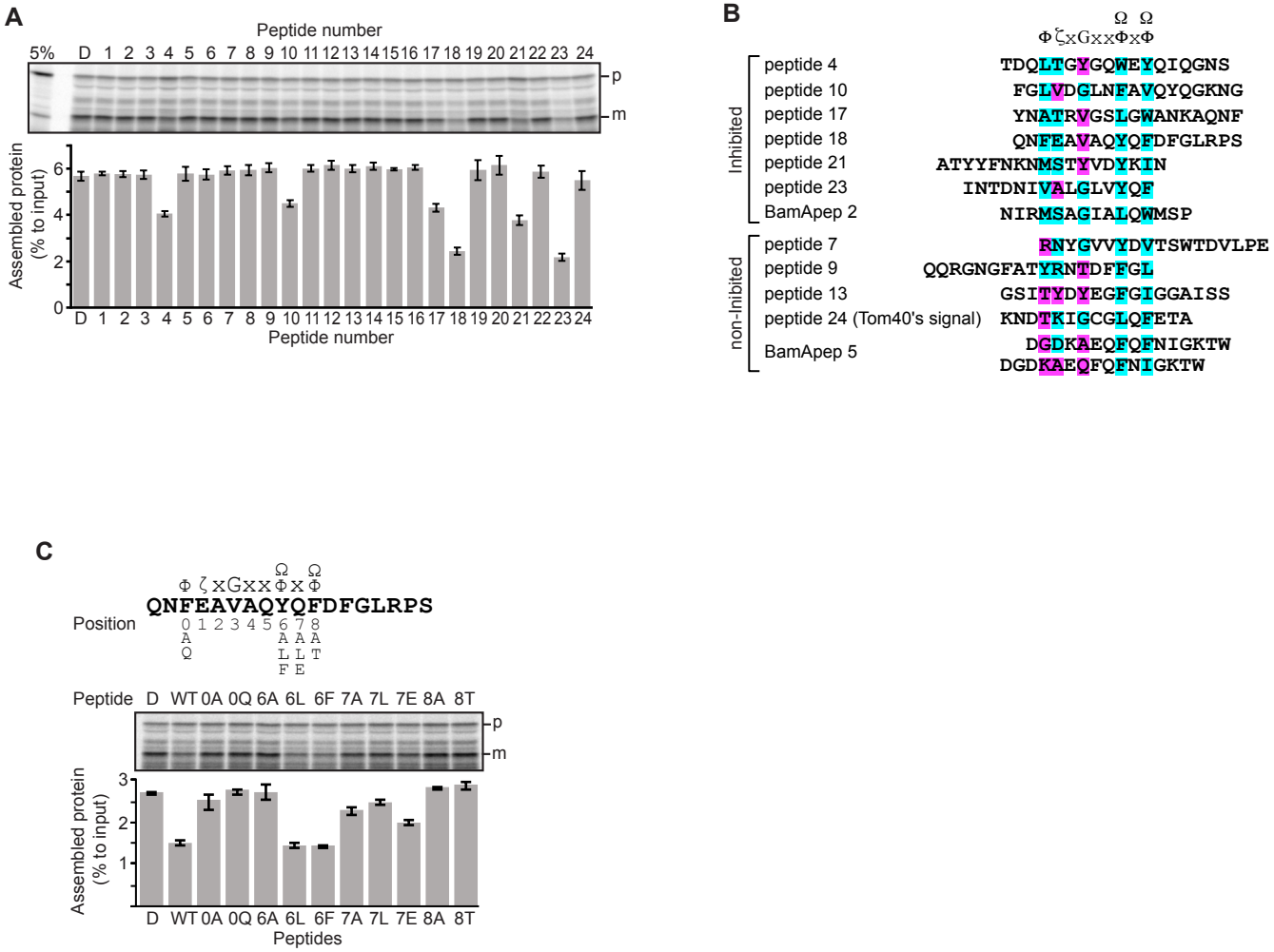

Figure 1

Germany et al. 2023

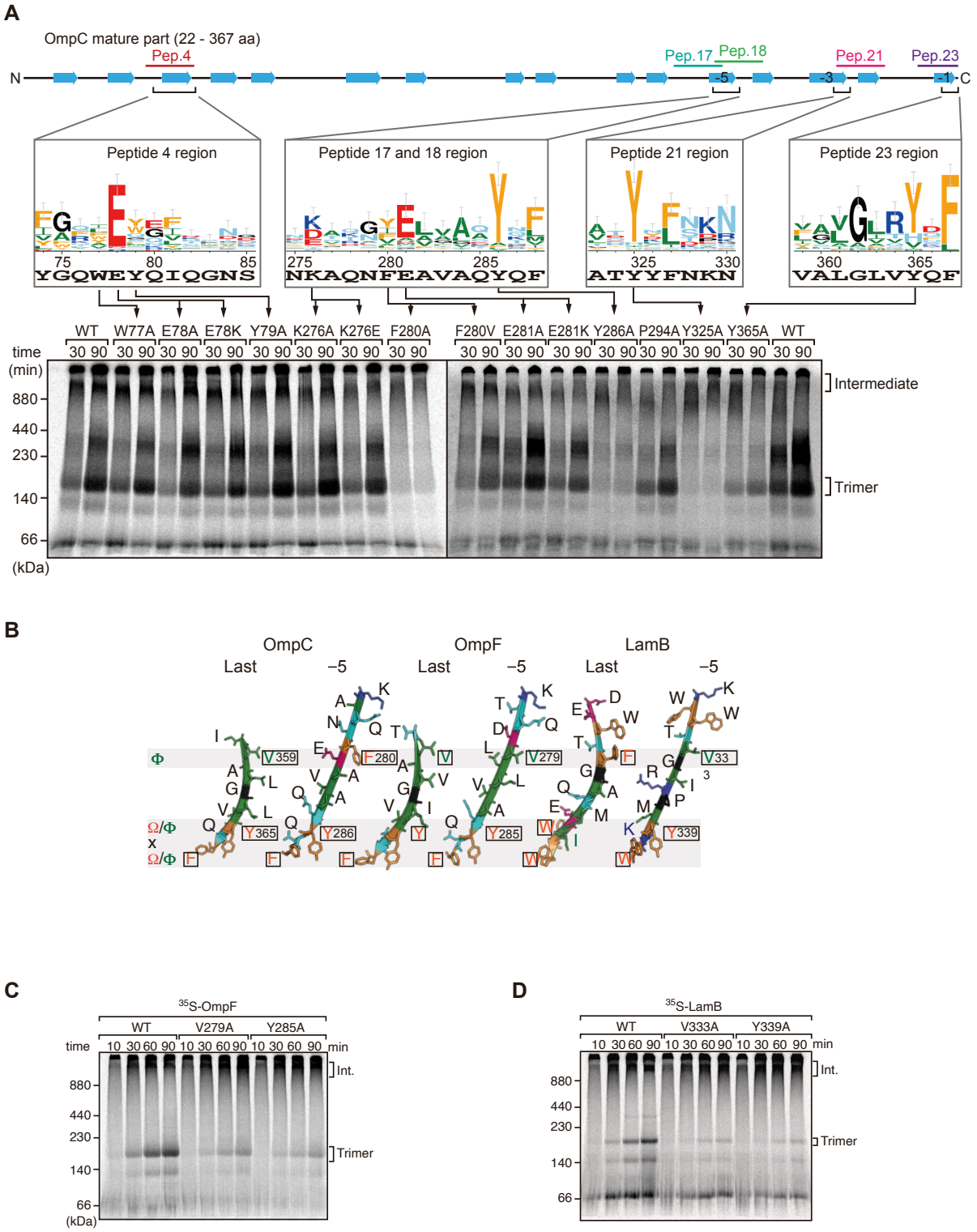

Figure 2

Germany et al. 2023

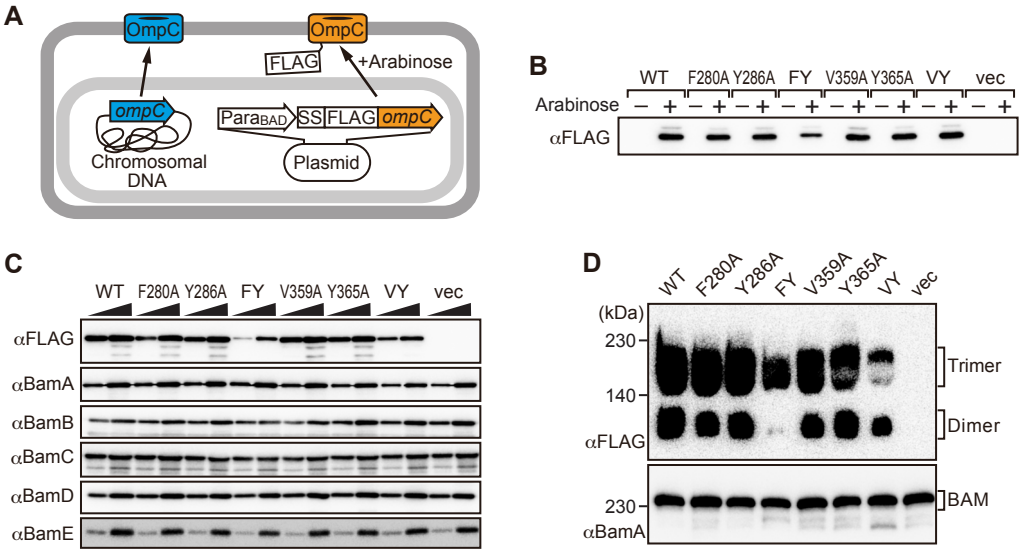

Figure 3

Germany et al. 2023

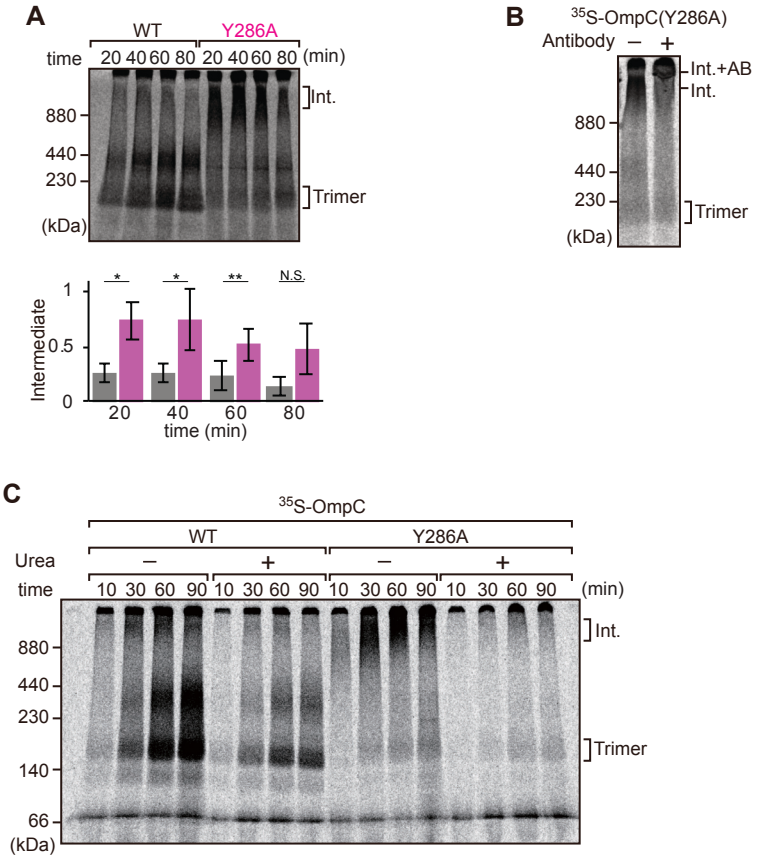

Figure 4

Germany et al. 2023

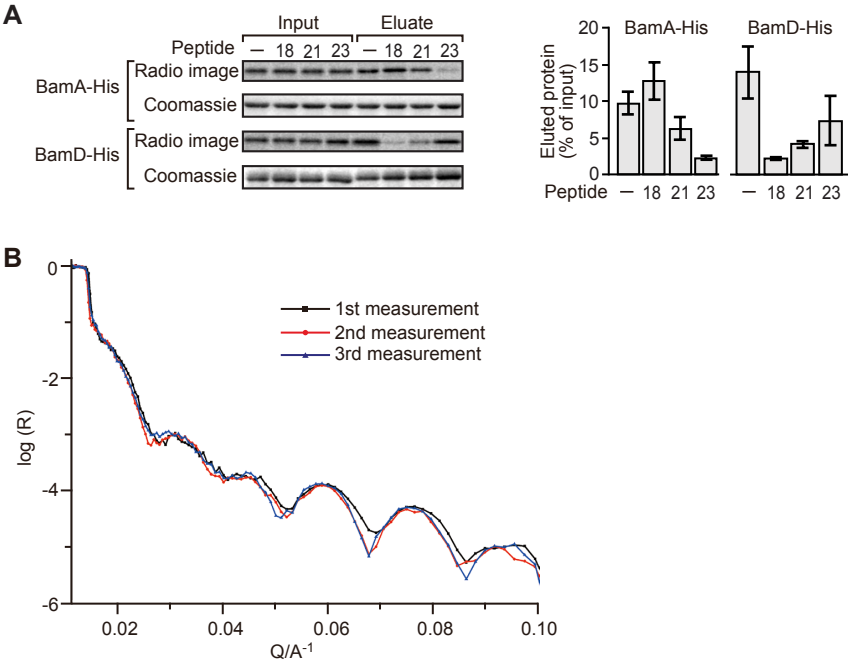

C

Layers	Thickness (Å) 1st measurement	Thickness (Å) 2nd measurement	Thickness (Å) 3rd measurement	Roughness (Å) 1st measurement	Roughness (Å) 2nd measurement	Roughness (Å) 3rd measurement
His_8	6.0±0.5	7.1±0.8	9.4±0.5	4.0±0.1	4.0±0.1	4.0±0.1
β-Barrel	56.9±1.5	58.7±0.4	56.8±1.5	10.1±0.1	12.6±1.8	6.0±0.1
P3-5	29.5±0.8	29.7±0.8	45.5±1.6	7.0±0.1	6.1±0.1	12.1±0.1
P1-2	31.2±0.8	30.3±0.4	28.5±0.9	13.8±0.1	13.7±0.1	5.0±0.1

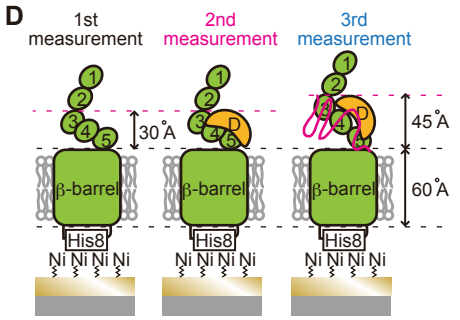

	Volume fraction (%) BamA 1st measurement	BamA 2nd measurement	BamA 3rd measurement	POPC 1st measurement	POPC 2nd measurement	POPC 3rd measurement	BamD 1st measurement	BamD 2nd measurement	BamD 3rd measurement	OmpC	Solution 1st measurement	Solution 2nd measurement	Solution 3rd measurement
His_8	---	---	---	---	---	---	---	---	---	---	25.3±7.4	25.8±7.0	22.7±1.7
β-Barrel	17.1±0.6	18.4±1.1	18.3±1.2	35.1±1.6	35.4±5.5	35.9±1.5	---	---	---	---	47.6±2.9	46.2±6.7	45.8±2.7
P3-5	10.7±0.9	11.0±0.8	11.7±2.9	3.4±1.7	3.3±0.5	3.3±0.9	8.8±1.1	9.0±3.3	8.0±1.2	---	85.9±2.6	76.9±2.0	76.0±7.3
P1-2	11.2±0.8	11.2±2.9	10.7±0.9	---	---	---	---	---	---	---	90.0±2.5	88.8±2.9	89.3±0.9

Figure 5 **Germany et al. 2023**

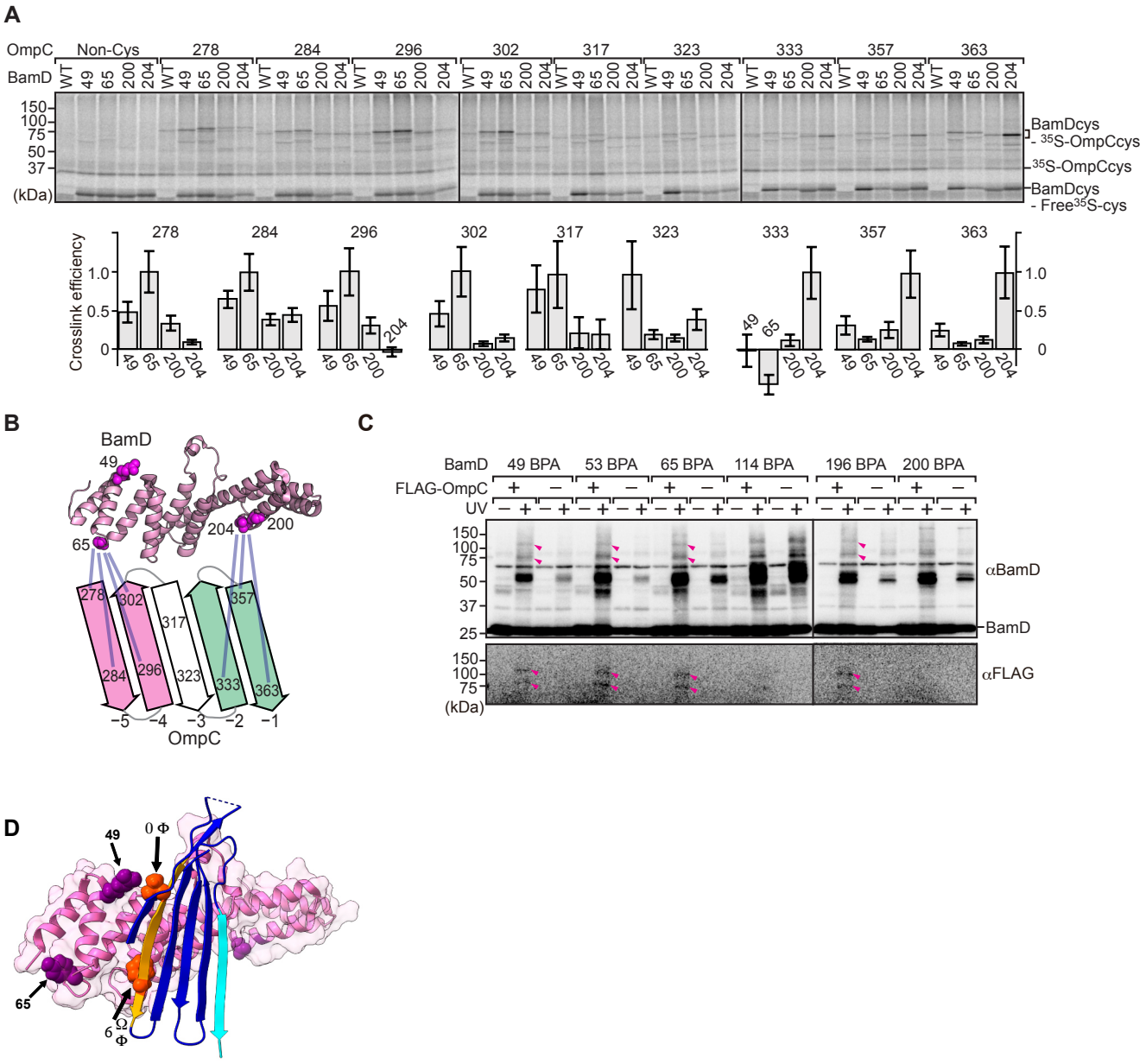

Figure 6

Germany et al. 2023

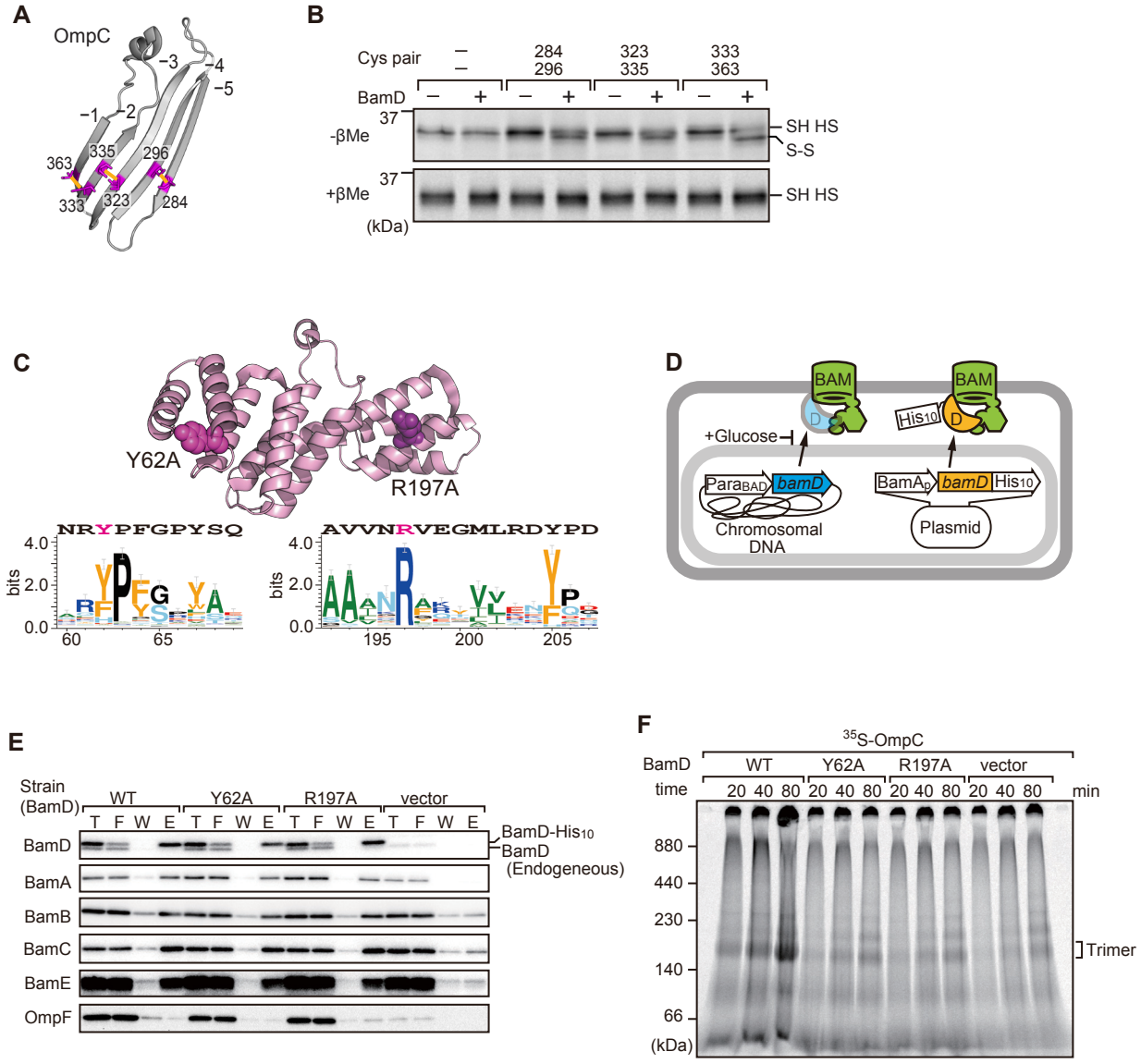

Figure 7

Germany et al. 2023

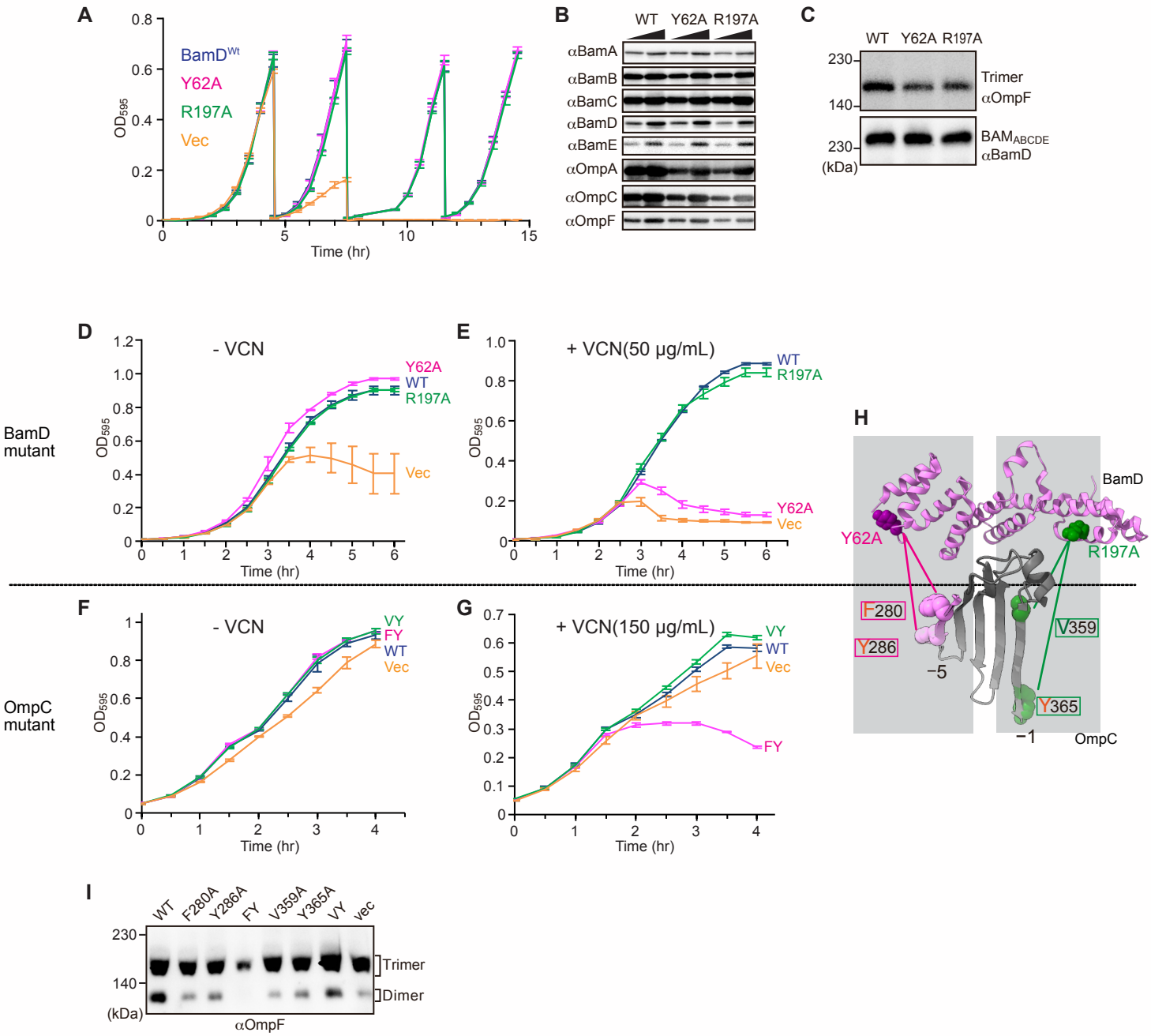

Figure 8

Germany et al. 2023

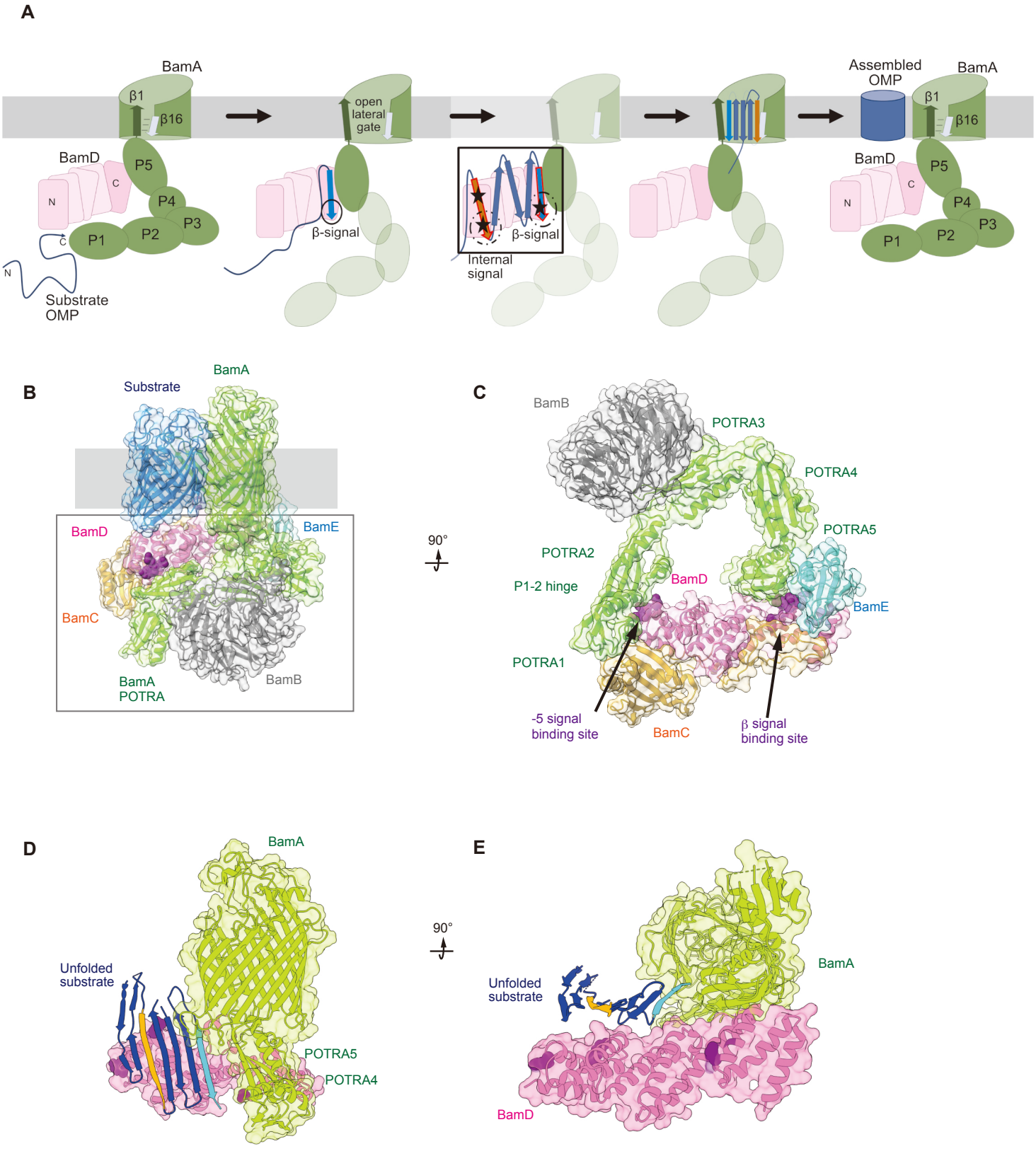

Figure 9 **Germany et al. 2023**